Materials Today Bio 24 (2024) 100919

Contents lists available at ScienceDirect

Materials Today Bio

journal homepage: www.journals.elsevier.com/materials-today-bio

Cadherin-responsive hydrogel combined with dental pulp stem cells and fibroblast growth factor 21 promotes diabetic scald repair via regulating epithelial-mesenchymal transition and necroptosis

Wenjie Lu [a,b], Juan Zhao [a,b], Xiong Cai [a,b], Yutian Wang [a,b], Wenwei Lin [a,b], Yaoping Fang [a,b], Yunyang Wang [a,b], Jinglei Ao [a,b], Jiahui Shou [a,b], Jiake Xu [a,c,d,**], Sipin Zhu [a,b,*]

[a] Department of Orthopaedics, The Second Affiliated Hospital and Yuying Children's Hospital of Wenzhou Medical University, Wenzhou Medical University, Wenzhou, Zhejiang, 325000 China
[b] School of Pharmaceutical Science, Wenzhou Medical University, Wenzhou, Zhejiang, 325000, China
[c] Shenzhen Institute of Advanced Technology, Chinese Academy of Sciences, Shenzhen, 518055, China
[d] School of Biomedical Sciences, University of Western Australia, Perth, Western Australia, 6009, Australia

ARTICLE INFO

Keywords:
Diabetic scald
Cadherin-responsive
Fibroblast growth factor 21
Epithelial-mesenchymal transition
Lysosomal stability

ABSTRACT

Diabetes causes a loss of sensation in the skin, so diabetics are prone to burns when using heating devices. Diabetic scalded skin is often difficult to heal due to the microenvironment of high glucose, high oxidation, and low blood perfusion. The treatment of diabetic scald mainly focuses on three aspects: 1) promote the formation of the epithelium; 2) promote angiogenesis; and 3) maintain intracellular homeostasis. In response to these three major repair factors, we developed a cadherin-responsive hydrogel combined with FGF21 and dental pulp stem cells (DPSCs) to accelerate epithelial formation by recruiting cadherin to the epidermis and promoting the transformation of N cadherin to E cadherin; promoting angiogenesis to increase wound blood perfusion; regulating the stability of lysosomal and activating autophagy to maintain intracellular homeostasis in order to comprehensively advance the recovery of diabetic scald.

1. Introduction

Skin is the first line of defense of the human body against the environment, which has functions such as resisting microbial invasion, maintaining body fluid and water balance, and regulating body temperature [1,2]. The main damage of scald injury is skin necrosis, and the high temperature could destroy the skin barrier function accompanied by a large amount of fluid exudation [3]. The repair of scald wounds is a very complex biological process, including the proliferation and migration of encapsulated cells, the deposition of collagen and extracellular matrix, and re-epithelialization [4]. Diabetes mellitus (DM) is a metabolic disease with persistent hyperglycemia, which can cause microvascular lesions in the body, resulting in disorders of blood circulation and nerve transmission, blunted sensation, and low sensitivity to heat [5]. Therefore, patients with DM often suffer from scalds due to improper use of heating equipment during heating [6]. In a state of high glucose, the blood perfusion and collagen deposition of the scald wound are reduced and epithelial keratinization becomes difficult, which could further delay wound healing [7,8]. Therefore, a scald with diabetes is a special type of pathological scald and requires a comprehensive remedy that can simultaneously improve the metabolic state of cells in the scalded area, promote angiogenesis, and potentiate epithelial keratinization in the state of high glucose.

Alginic acid is a naturally occurring polysaccharide that forms various alginates by combining with different cations present in seawater [9]. Sodium alginate exhibits convenient gelation, high affinity towards biological systems, excellent drug delivery capabilities, and remarkable water absorption properties, making it highly valuable for applications in biomedical engineering [10]. Sodium alginate can coordinate with free calcium ions to form a three-dimensional network structure of calcium alginate hydrogel. The degree of cross-linking

* Corresponding author. Department of Orthopaedics, The Second Affiliated Hospital and Yuying Children's Hospital of Wenzhou Medical University, Wenzhou Medical University, Wenzhou, Zhejiang, 325000, China.
** Corresponding author. Department of Orthopaedics, The Second Affiliated Hospital and Yuying Children's Hospital of Wenzhou Medical University, Wenzhou Medical University, Wenzhou, Zhejiang, 325000, China.
E-mail addresses: Jiake.xu@uwa.edu.au (J. Xu), sipinzhu@163.com (S. Zhu).

https://doi.org/10.1016/j.mtbio.2023.100919
Received 19 September 2023; Received in revised form 15 December 2023; Accepted 15 December 2023
Available online 22 December 2023

Abbreviations

Gel	Cadherin-responsive hydrogel
FGF21	Fibroblast growth factor 21
DPSC	Dental pulp stem cells
DM	Diabetes mellitus
EMT	Epithelial-mesenchymal transition
FBS	Fetal bovine Serum
NDI	N-dodecylimidazole
HRP	Horseradish peroxidase
ECL:	Enhanced chemiluminescence
HEPES	4-(2-Hydroxyethyl)piperazine-1-ethanesulfonic
EDS	Energy dispersive spectrometer
RBCs	Red blood cells
PBS	Phosphate Buffered Saline;
IP	Intraperitoneal injection
BCA	Bicinchoninic acid
PVDF	Polyvinylidene fluoride;
TBST	Tris-Buffered Saline and Tween 20
DMSO	Dimethyl sulfoxide;
DPBS	Dulbecco's Phosphate Buffered Saline;
TBHP	*Tert*-butyl Hydroperoxide.

between sodium alginate and calcium ions increases with the concentration of the calcium solution [11]. Calcium ions are essential trace elements in the human body and pose no harm [12].

Epithelial-mesenchymal transition (EMT) is a key biological process that regulates epithelial keratinization, and is characterized by the switch of N cadherin and E cadherin [13,14]. Research has demonstrated that epidermal keratinocytes undergo a phenotypic shift from an epithelial to a mesenchymal state during skin wound healing, resulting in the manifestation of EMT characteristics [15]. In the context of wound epithelium reformation, cell adhesion and gap junction mediating cell surface protein E cadherin play a crucial role in maintaining the integrity of the epithelial cytoskeleton and regulating cellular polarity, differentiation, growth, and migration [16]. Cadherin is a Ca^{2+} dependent cell adhesion glycoprotein. The expression level and effect strength of cadherin are closely related to calcium ion concentration. Recently, alginate has also been reported to be able to bind calcium ions into hydrogels to up-regulate N cadherin and E cadherin expression at the injury junction while avoiding calcium overload [17]. Therefore, whether cadherin-responsive hydrogels can promote EMT to facilitate epithelialization has aroused great interest.

In diabetic conditions, the high glucose environment in the body often increases the endogenous oxidative stress response, resulting in cell membrane organelles being affected [18,19]. Therefore, a drug with hypoglycemic function is needed to regulate the high glucose internal environment and improve the metabolic efficiency of cells while protecting cells [20]. Fibroblast growth factor 21 (FGF21) is a growth factor with glucose and lipid metabolism function first discovered in mouse embryos [21]. Studies have shown that FGF21 can regulate gluconeogenesis, increase peroxisome activity, and modulate metabolism in vivo [22,23]. Recent studies have confirmed that FGF21 has the ability to promote lysosomal stabilization and enhance autophagy, however, whether FGF21 can regulate the repair of diabetic scald skin through autophagy pathway is not clear [24,25].

Dental pulp stem cells (DPSCs) are fibroblasts derived from dental pulp tissues, which have the ability of self-renewal and multi-directional differentiation [26]. DPSCs have attracted great attention in stem cell therapy in recent years due to their abundant sources, low immune rejection property and no ethical controversy [27]. It is evident that the diabetic blood vessels often shrink due to high glucose and high oxidation microenvironment, and blood perfusion is significantly reduced accompanied with slow recovery of the scald. Studies suggest that DPSCs might have their ability to differentiate into endothelial cells, effectively promote the regeneration of the blood vessels, and tolerate high glucose environment to promote scald wounds of angiogenesis [28,29].

Therefore, in this study, we designed a therapeutic system combining DPSCs and FGF21 in cadherin-responsive hydrogel to treat diabetic scald by regulating EMT and necroptosis, as well as promoting angiogenesis and epithelialization.

2. Experimental section

2.1. Materials

3T3-L1 cells were supplied by OTWO (Shenzhen, China). Fetal bovine Serum (FBS) and RPMI 1640 medium (1640) were obtained from Gibco (California, USA). D-(+)-Glucose Solution (20 %, sterile) was obtained from Beyotime Biotechnology (Shanghai, China). FGF21, CAY10650, and 1-Dodecylimidazole (NDI) were bought from MedChemExpress (New Jersey, US). Primary antibodies against CTSD (69854S), C-CASP8 (8592S), and β-catenin (8480S) were purchased from Cell Signaling Technology (US). Primary antibodies against P62 (ab109012) and N-cadherin (ab98952) were supplied by Abcam (Cambridge, UK). Primary antibodies against α-SMA (701457) were obtained from Thermo Fisher Scientific (Massachusetts, US). Primary antibodies against LC3B (A17424) were obtained from ABclonal (US). Primary antibodies against E-cadherin (AF0131) were bought from affinity (OH, US). Primary antibodies against α-Tubulin (R23454), β-actin (R23613), anti-mouse and anti-rabbit secondary antibodies IgG-conjugated with horseradish peroxidase (HRP) and Ultrasensitive enhanced chemiluminescence (ECL) kit were obtained from ZenBioScience (Chengdu, China). Donkey Anti-Rabbit/Mouse IgG H&L (Alexa Fluor® 488) pre-adsorbed, Donkey Anti-Rabbit/Mouse IgG H&L (Alexa Fluor® 647) pre-adsorbed were obtained from Abcam (Cambridge, UK).

2.2. Synthesis and characterization of hydrogel

2.2.1. Synthetic method

0.05 g sodium alginate (Sigma-Aldrich, St Louis, Missouri, US) and 10 μg FGF21 (MedChemExpress, New Jersey, US) were dissolved in 1 mL 150 mM NaCl and 20 mM HEPES, free acid (pH 7.4) (Beyotime Biotechnology, shanghai, China) to form solution A. Then, 1×10^6 DPSCs were dyed by CM-DiI (Invitrogen, California , US) that resuspended in solution A to form homogeneous solution B. Then we evenly spread solution B in the culture dish and added 1 mL 100 mM $CaCl_2$ and 10 mM HEPES, free acid (pH 7.4). Let the solution incubated for 10 min. The excess solution was then sucked up, and 2 ml 150 mM NaCl and 10 mM HEPES, free acid (pH 7.4) was added for washing. The washing process lasted for 2 min, 3 times in total. The material produced by the above process is cadherin-responsive hydrogel combined with DPSCs and FGF21. Gel means that FGF21 and DPSCs were not added in the simple gelation of sodium alginate and calcium, and Gel + FGF21 means that FGF21 was added in the simple gelation without DPSCs. In subsequent animal experiments, we used tools to divide the hydrogels into round materials with a diameter of 6 mm. The round material of Gel + DPSC group and Gel + DPSC + FGF21 group consisted of 1×10^4 DPSCs.

2.2.2. Characterization and testing of materials

2.2.2.1. The microstructure of the hydrogels and Ca^{2+} atomic energy. The morphology of the hydrogels was detected by scanning electron microscopy (SEM, Nova 200 NanoSEM, FEI, USA). Ca^{2+} atomic content and distribution of Gel and Gel + FGF21 were quantified by energy dispersive spectrometer (EDS) (NOVA 200 NANOSEM, FEI, US). The chemical structure of hydrogels was detected by fourier transform

infrared spectroscopy (FITR, Thermo, NICOLET is20).

2.2.2.2. Drug release. At 0 h, 6 h, 12 h, 18 h, 24 h, 36 h, 48 h, 60 h, 72 h, 96 h,108 h, 120 h,132 h,144 h, 156 h, 168 h, we replaced cadherin-responsive hydrogel with FGF21 with a new medium and then collected the previous medium. The collected medium at each time point was detected by enzyme-linked immunosorbent assay Kit (ELISA kit). The following parameters and designations were used: Accumulative released FGF21(%) = ODx/OD × 100 %. ODx = ODt + Ax; ODx: Absorbance of cumulative release of FGF21 at time point X; ODt: Absorbance of FGF21 cumulative release at the previous time point of X time point; AX: Absorbance of FGF21 released at X time point; OD: Absorbance of control group; X = 2, 6, 12, 18, 24 h etc. For example: OD2 = OD2, OD4 = OD2+A4.

2.2.2.3. Mechanical properties and gelling properties of materials. We used a universal testing machine (INSTRON, Massachusetts, US) to test the mechanical properties of materials. Materials were made into a cylinder with a diameter and a height of about 5 mm, and 1000 N was applied to it. The moving speed of the machine was 1 mm/min. Finally, the results were analyzed by GraphPad Prism 8.4.0, GraphPad Software. The rheological properties of the hydrogels were determined by the Thermo Fisher HAAKE MARS rheometer.

2.2.2.4. Hemolysis test. We gently mixed the PBS solution containing small particles of cadherin-responsive hydrogel with 5 % v/v red blood cells (RBCs) in a volume ratio of 1:1. We centrifuged the sample that was left at room temperature for 30 min at 3000 rpm, 4 °C for 7 min, and then took out the supernatant. 150 μl supernatant was transferred to 96 well plate and measured with the absorbance at 540 nm. The negative control was the same amount of PBS solution, and the positive control was the same amount of deionized water. The following parameters and designations were used. Hemolysis (%) = (As−Ab)/(Ap−Ab) × 100 %; As: sample absorbance, Ab: negative control (PBS), Ap: positive control (deionized water).

2.2.2.5. In vitro degradation properties of the hydrogel. Prior to the experiment, a specific weight of dry gel (W1) was measured and then mixed with PBS buffer before being placed on a shaker at 37 °C and 60 r/min. The solution was changed every other day, and at predetermined time points, the gel was removed, dried at 65 °C until constant weight (W2), and weighed multiple times. The degradation rate was calculated using the formula: W2/W1.

2.2.2.6. Measurement of the cytotoxicity of cadherin-responsive hydrogel. 3T3-L1 cells were divided into two groups: the control group and the cadherin-responsive hydrogel co-culture group. Only complete medium was added to the control group, and 5 mg of cadherin-responsive hydrogel fragments per mL of medium was added to the cadherin-responsive hydrogel co-culture group. One day after co-culture, the cells were digested with trypsin and then examined for cell survival using the Calcein/PI kit (Beyotime Biotechnology, shanghai, China). After incubation, we tested the results at the excitation wavelength of 488 and 560 nm. Green fluorescence represents living cells, and red fluorescence represents dead cells.

3T3-L1 cells were enumerated and evenly distributed into 96-well plates, with a cell count ranging from 8000 to 10000 per well. The cells were randomly divided into the following groups: control group, 50 mM Ca^{2+} group, 100 mM Ca^{2+} group and 150 mM Ca^{2+} group, 50 mM Ca^{2+} gel group, 100 mM Ca^{2+} gel group, 150 mM Ca^{2+} gel group. After the cells were completely adherent, 90 μl complete medium and 10 μl $CaCl_2$ solution were added to each well in the Ca^{2+} group, and the same volume of PBS was added to each well in the control group. The Ca^{2+} gel group was taken from the leaching solution (1 cm^3 hydrogel was dissolved in 10 ml complete medium for 24 h), and then 100 μl of the leaching solution was added to a 96-well plate, and the same amount of medium was added to the control group. After 24 h, the absorbance of cells in each group was measured at a wavelength of 450 nm using CCK8, followed by conversion to determine the cell viability.

2.3. Animals and experimental model

All experimental procedures and animals comply with experimental animal ethics. One hundred and ninety C57BL/6 male mice (20–22 g) were obtained from the Experimental Animal Center of Wenzhou Medical University.

2.3.1. Normal control mice

In a preliminary experiment, we divided 60 experimental animals into six groups, which were the control group, the burn group, the Gel group, the Gel + FGF21 group, the Gel + DPSC group, and the Gel + DPSC + FGF21 group. All animals lived in a suitable environment, where they could get food and water at any time. The surgical environment was cleaned and disinfected before surgery. Mice were injected with 1 % sodium pentobarbital (50 mg/kg, IP). We set the temperature control scald instrument (YiYan Scientific, Jinan, China) to 80 °C for 11 s. An identical burn area appeared on each mouse with the same location and surgical means. We applied hydrogel of the same size to the wound and covered with Tegaderm films (3 M, USA). The outermost layer is covered with a medical bandage. Mice were euthanized after 14 days. In 0 days, 7 days, and 14 days, the appearance of the mice was taken with a digital camera.

2.3.2. Diabetic mice

Seventy healthy mice were injected with 150 mg/kg Streptozotocin. After 20 days, we selected mice with blood glucose higher than 16.7 mmol/L. We divided the experimental animals into six groups: the control group, the burn group, the Gel group, the Gel + DPSC group, the Gel + DPSC + FGF21 group. The following modeling and testing methods were consistent with normal control mice.

2.3.3. Diabetic mice used for mechanism research

Thirty mice with the cadherin-responsive hydrogel containing FGF21 and DPSCs were randomly divided into three groups: the control group, the Gel + DPSC + FGF21+NDI (MedChemExpress, New Jersey, US) group, and the Gel + DPSC + FGF21+CAY10650 (MedChemExpress, New Jersey, US) group. Ten mice were intraperitoneally injected with 2.5 mg/kg CAY10650 for 10 days, and ten mice were intragastric administration with NDI for 10 days. The following modeling and testing methods were consistent with normal control mice.

Thirty mice without hydrogel application were randomly divided into three groups: the control group, the burn group, and the CAY10650 group. Ten mice were intraperitoneally injected with 2.5 mg/kg CAY10650 for 10 days. The following testing methods are the same as above.

2.4. H&E staining and masson trichromatic staining

We used 4 % paraformaldehyde to fix the tissues. The gradient alcohol was dehydrated, and the tissue was sectioned into a 5 μm slice with paraffin. After H&E staining and Masson trichromatic staining, the sections were imaged by a light microscope (x 10) to measure the healing degree of the wound. The skin with unclear hair follicle structure and no complete epithelium was defined as the skin without healing.

2.5. Western blot (WB)

We added the treated skin tissue to the tissue lysis buffer at the ratio of 100 mg/700 μL. The tissues were homogenized with a grinder (JingXin, Shanghai, China) after incubating on the ice for half an hour.

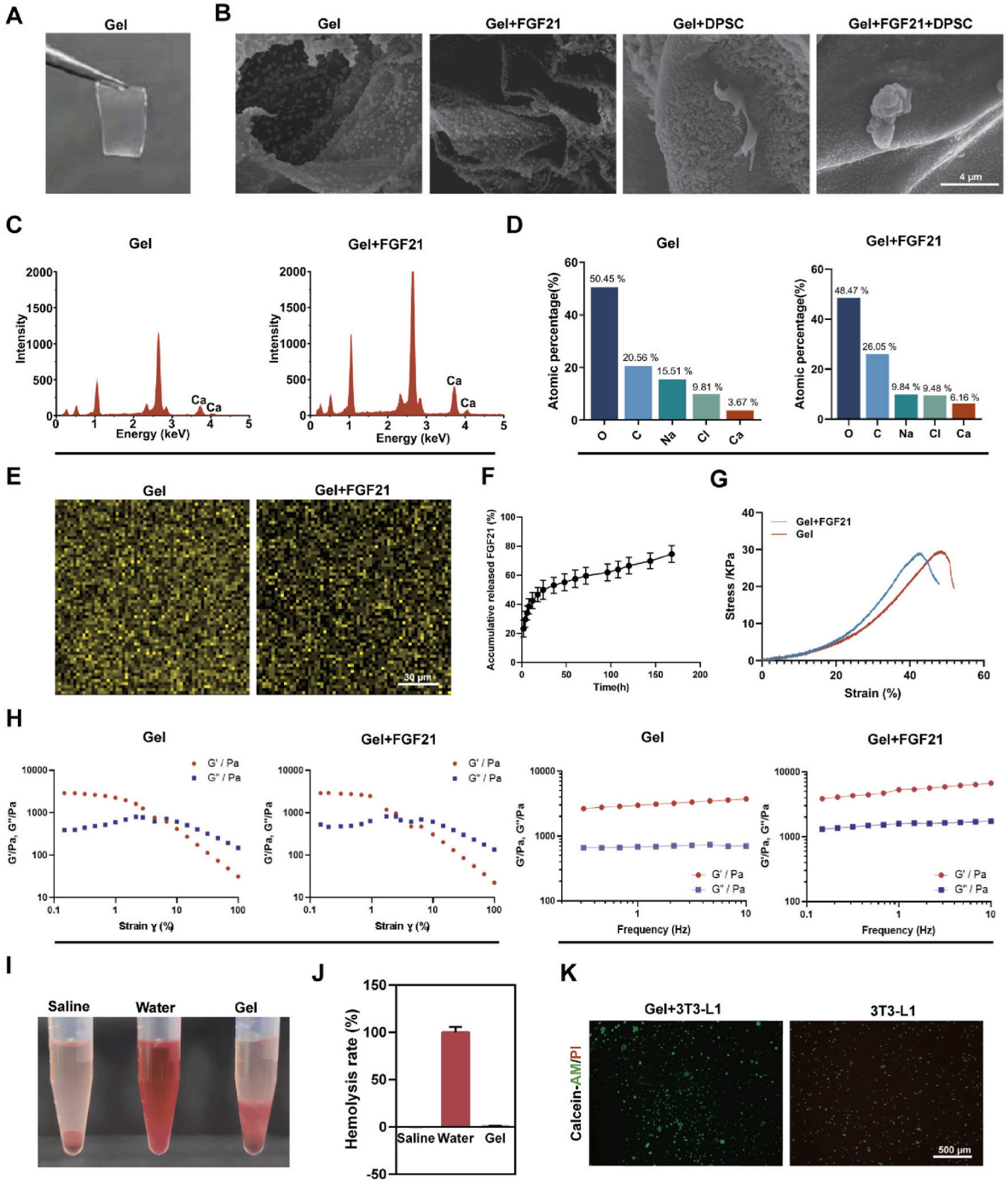

Fig. 1. Characterization of the cadherin-responsive hydrogel. (A) Morphological display of cadherin-responsive hydrogel. (B) Scanning electron microscope images of hydrogels in different groups. Scale: 4 μm. (C) The Ca^{2+} atomic content of Gel and Gel + FGF21 samples were quantified by energy dispersive spectrometer. (D) Element constituents in Gel and Gel + FGF21 samples (atomic percentage) by energy dispersive spectrometer. (E) Ca^{2+} distribution results of Gel and Gel + FGF21 samples by energy dispersive spectrometer. (F) The release profile of FGF21 from the hydrogel. (G) A stress-strain curve was obtained using the universal mechanical testing machine. (H) Rheological characterization of hydrogel strain sweep, and frequency sweep analyses. (I) Pictures from the hemolytic activity test of the hydrogel. (J) Hemolytic percentage of the hydrogel. (K) Live/dead staining of 3T3 cells seeded on hydrogel after a 24 h culture. Live cells (green); Dead cells (red). Magnification: 4X; Scale: 500 μm.

The homogenized liquid was centrifuged at 4° for 15 min at 12000 revolutions and repeated twice. The supernatant of fluid was then retained. The bicinchoninic acid (BCA) reagents (Thermo, Rockford, IL, USA) was used to unify the protein concentration of 40 μg in 10 μL. Finally, we added 5 × loading buffer and pure water to the supernatant and heated it at 100 °C for 5 min. We used a microinjection needle to load 10 μ L of protein into the swimming lane of 10 % gels, separated the protein and transferred it to the PVDF membrane (Bio-Rad, Hercules, CA, USA). Subsequently, the PVDF membrane was sealed with 10 % skimmed milk (Bio-Rad) for 1 h and washed with TBST three times. We incubated the membrane with the corresponding primary antibody at 4° for 12–16 h. The membrane was washed three times by TBST and incubated with secondary antibody at room temperature for 1 h. Finally, we used TBST to wash the membrane three times and used The

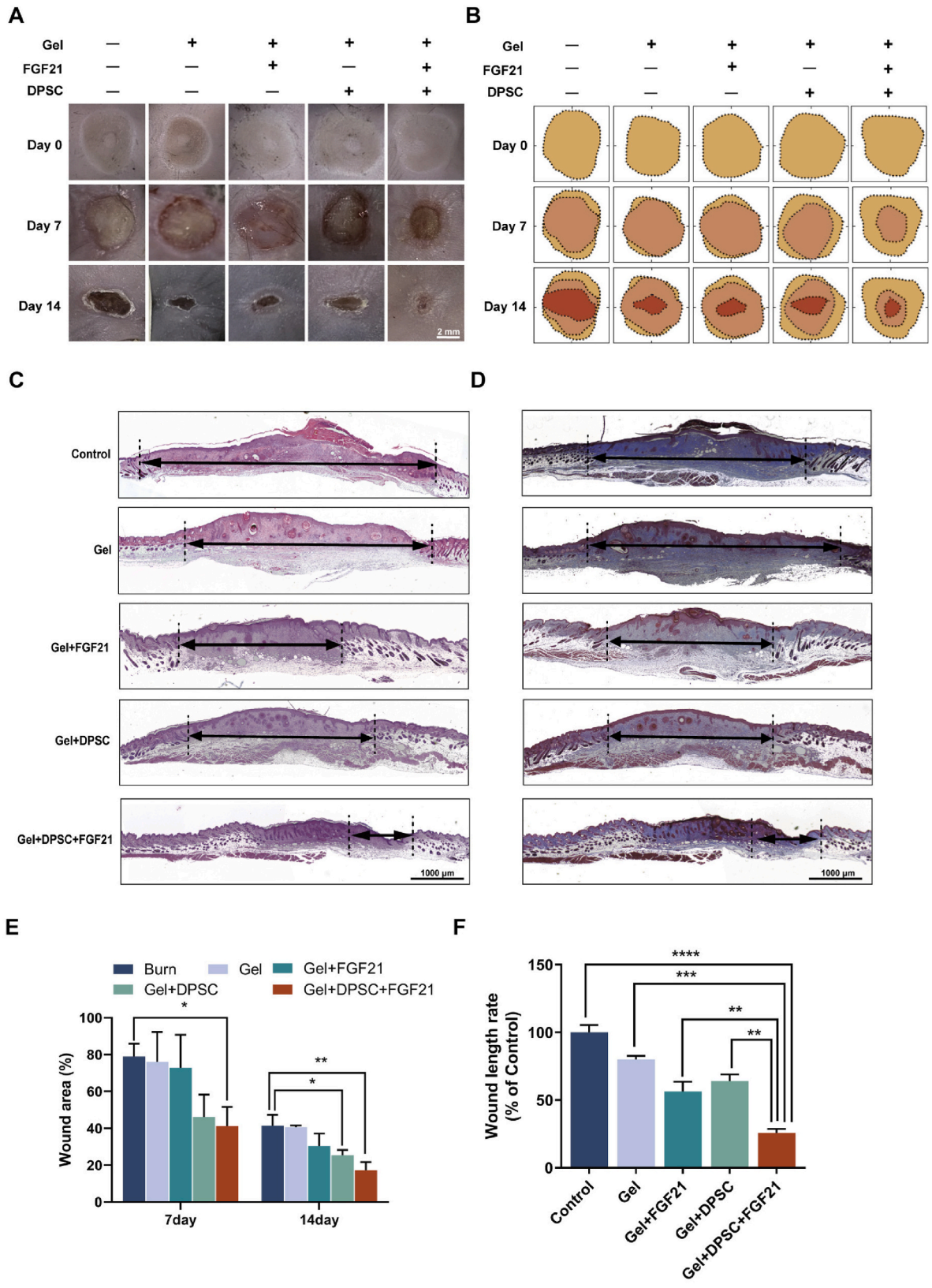

Fig. 2. Wound closure of Gel + DPSC + FGF21 treatment in normal control mice. (A) Photographs of four types of treated wounds on day 0, 7, 14. Scale: 2 mm. (B) Simulation plots. (C, D) Images of H&E and Masson staining of wound after 14 d of treatments. Scale: 1000 μm. (E) Quantitative analyze of the wound area. (F) Quantitative analysis of the wound length rate. * represents $P < 0.05$. ** represents $P < 0.01$. *** represents $P < 0.001$. Data are represented as mean ± SD (n = 3).

ChemiDoc XRS$^+$ Imaging System (Bio-Rad) to record the experimental results.

2.6. Immunofluorescence (IF)

Slices of paraffin were eluted and washed with PBS, which was applied for antigen retrieval (3min, 100 °C) with citrate buffer solution. The corresponding primary antibody incubation is carried out for 12–16 h at 4 °C. Anti-fluorescence quenching sealing solution (Yeasen Biotechnology, Shanghai, China) containing DAPI was applied to the tissue, and the tissue slice was then processed with a cover slip. Nikon laser confocal microscope (Nikon, Japan) was used to record the fluorescence result.

2.7. Culture of DPSCs and 3T3-L1

2.7.1. Isolation and culture of DPSCs

Wenzhou Medical University (No. wykq-2018-008SC) approved the following DPSCs experiments. The teeth were obtained the third molars of volunteers without oral diseases. An informed consent of the volunteers whose teeth were extracted was included as an attachment 1. We disinfected the removed teeth and cut them into small pieces with a mechanical knife. Then we used 4 mg/mL dispase (Sigma-Aldrich, St. Louis, MO, USA) and 3 mg/mL collagenase type I (Gibco, USA) to completely digest the tissue in a 37-degree incubator for 30 min. The extracted cells were resuspended and cultured in a primary mesenchymal stem cell culture system (iCell, Shanghai, China).

2.7.2. CM-DiI staining of DPSCs

50 μg CM-Dil was dissolved in 50 μL DMSO to obtain a solution with a concentration of 1 mg/mL. After being digested, the cells were centrifuged at 1000 rpm for 5 min. After pouring out the culture medium, the cells were resuspended with 1 mL Dulbecco's Phosphate Buffered Saline (DPBS). Then cells were added 2 μl CM-DiI dye and incubated at room temperature for 5 min and then 4 °C for 15 min. The cells were centrifuged at 1000 rpm for 5 min, then resuspended with DPBS, and centrifuged again at 1000 rpm for 5 min.

2.7.3. Culture of 3T3-L1 cells

We cultured 3T3-L1 cells in 33 mmol/L glucose and 10 % serum for one week. Then the cells in the high glucose state were divided into four groups, namely the control group, the TBHP group (added 100 nM TBHP), the FGF21 group (added 0.375 nM FGF21), and the FGF21+TBHP (added 100 nM and 0.375 nM FGF21. After giving FGF21 for 12 h, TBHP was used to stimulate for 12 h. We took out cells and isolated proteins from cells for the WB test.

2.7.4. CCK-8 test of 3T3-L1 cells

3T3-L1 cells with a density of 5000 cells/well were seeded on 96 well plates. After 24 h, the cells were divided into six groups: the control group, the 20 nM TBHP group, 50 nM TBHP group, 100 nM TBHP, 120 nM TBHP and 200 nM TBHP group. After 12 h, all wells were added with CCK8 solution and detected at 450 nm wavelength after 2 h.

2.8. Statistical analyses

The present form of the experimental results was expressed as means ± SEM. Statistics software included Excel, ImageJ and GraphPad Prism 8. One-way analysis of variance (ANOVA) was used in a statistical analysis, and statistical difference with a P value < 0.05 was considered significant.

3. Results and discussion

3.1. Characterization of the cadherin-responsive hydrogel

The excessive presence of Ca^{2+} induces cell death. Therefore, we initially screened hydrogels with optimal performance from gels formed using $CaCl_2$ solutions at varying concentrations. Mechanical testing revealed that the compression modulus of the hydrogel increased proportionally with increasing Ca^{2+} concentration (Sfig 1A-B). Subsequently, we evaluated the degradation performance of the hydrogel and observed a slower degradation rate within the first 7 days as Ca^{2+} concentration increased (Sfig 1C). Fourier transform infrared spectroscopy experiments demonstrated a decrease in peak intensity with increasing Ca^{2+} concentration (Sfig 1D). Furthermore, CCK8 test results indicated that while a standalone use of 50 mM $CaCl_2$ caused significant cellular damage, a concentration of 150 mM was required to induce damage after incorporating it into the hydrogel system (Sfig 1E-F). According to the above results, 100 mM $CaCl_2$ solution was selected as the gelling liquid.

We successfully prepared the cadherin-responsive hydrogel by combining alginate with calcium ions (Fig. 1A) and detected the microstructure of the hydrogel by scanning electron microscopy. The experimental results showed that the cadherin-responsive hydrogel had a good pore structure, and the pore structure was also preserved after being coated with FGF21. In Gel + DPSC and Gel + DPSC + FGF21 groups, it was observed that DPSC could survive in the pores of hydrogels (Fig. 1B). We then used energy dispersive spectroscopy (EDS) to identify the presence of metal ions. The experiment showed that there were five elements of C, O, Na, Cl, and Ca ions participated in the composition of the cadherin-responsive hydrogel and was distributed evenly (Fig. 1C–E). To verify the ability of cadherin-responsive hydrogels to release FGF21 slowly, we performed an FGF21 release assay, and the results showed that FGF21 was released slowly within 7 days (Fig. 1F). Skin is a relatively soft tissue, and biomaterials with excessive hardness could cause skin to slow down the repair process [30]. We tested the compression modulus of cadherin in response to hydrogel, and the experimental results showed that the hydrogel was relatively soft (Fig. 1G). Finally, the gelling properties of hydrogels were detected by rheometer, and the results showed that cadherin hydrogels could maintain gel properties stably (Fig. 1H). After testing the physicochemical properties of the hydrogels, hemolysis test and calcein/PI staining were used to identify the bio-affinity of the hydrogels. The experimental results showed that the hydrogels had a good bio-affinity without causing hemolysis and almost no toxicity to cells (Fig. 1I–K). When the hydrogel was applied to the scald wounds of mice, no significant lesions were observed in the parenchymal organs of the mice (Sfig 2). In summary, the constructed hydrogel has good physical and chemical properties and is suitable for skin repair.

3.2. Cadherin-responsive hydrogel combined with DPSCs and FGF21 promotes scald repair in normal mice

To investigate the effect of cadherin-responsive hydrogel combined with DPSCs and FGF21 on scald wound repair, we applied it to the mouse scald model and recorded the recovery of scald in each group at 0, 7, and 14 days. The experiment results showed that the cadherin-responsive hydrogel combined with DPSCs and FGF21 system had the best effect of repair. After 14 days, the scald wounds of mice were nearly completely repaired and no obvious scar formation was found (Fig. 2A–B, E). Then we used H&E staining to observe the structural details of the recovered tissue in the scald area. The cadherin-responsive hydrogel combined with DPSCs and FGF21 was found to reduce the damaged area compared with other groups, and the repaired area had significant hair follicle growth (Fig. 2C, F). At the same time, Masson staining was used to detect the collagen deposition, and the results showed that the Gel + DPSC + FGF21 group had the best collagen

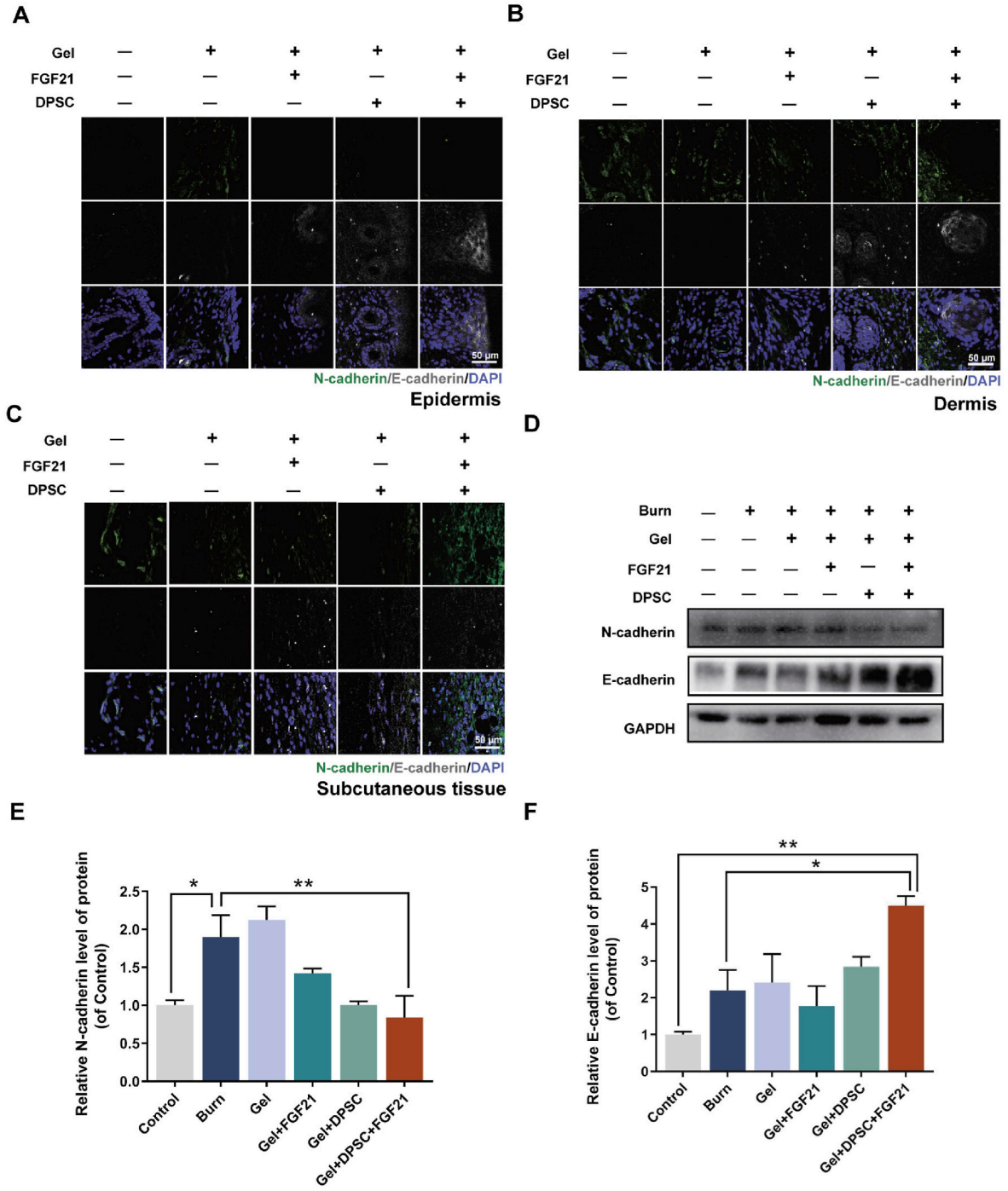

Fig. 3. Gel + DPSC + FGF21 promotes the transition of N cadherin to E cadherin in normal control mice. (A–C) Immunofluorescence showing the expression of N-cadherin (green), E-cadherin (white) in different groups in the epidermis, dermis and subcutaneous tissue. The nuclear is labeled by DAPI (blue). Scale: 50 μm. (D–F) Representative images and analysis of western blots of N-cadherin and E-cadherin in the indicated groups. GAPDH was used as a reference. * represents $P < 0.05$. ** represents $P < 0.01$. Data are represented as mean ± SD (n = 3).

recovery (Fig. 2D). These results confirmed that the system of cadherin-responsive hydrogel combined with DPSCs and FGF21 could effectively promote the repair of scald wound.

3.3. Cadherin-responsive hydrogel combined with DPSCs and FGF21 regulates epithelial EMT

Skin is the first barrier against the invasion of viruses and bacteria, and epithelial integrity plays a crucial role in the skin barrier function [31]. After scald, the epithelium is severely damaged, so it is particularly important to effectively promote the formation of epithelium [32]. The formation of epithelium is closely related to the effect of E cadherin, and the expression of E cadherin is often down-regulated after injury [33], whereas N cadherin is often up-regulated after skin injury [34]. EMT is characterized by a loss of epithelial cell markers with the upregulation of N-cadherin, followed by the emerging of mesenchymal cell markers with the downregulation of E-cadherin, which is involved in the biological processes of skin healing [35]. Therefore, whether cadherin-responsive hydrogel combined with DPSCs and FGF21 can regulate the cadherin switching of N cadherin to E cadherin in response to hydrogel is of

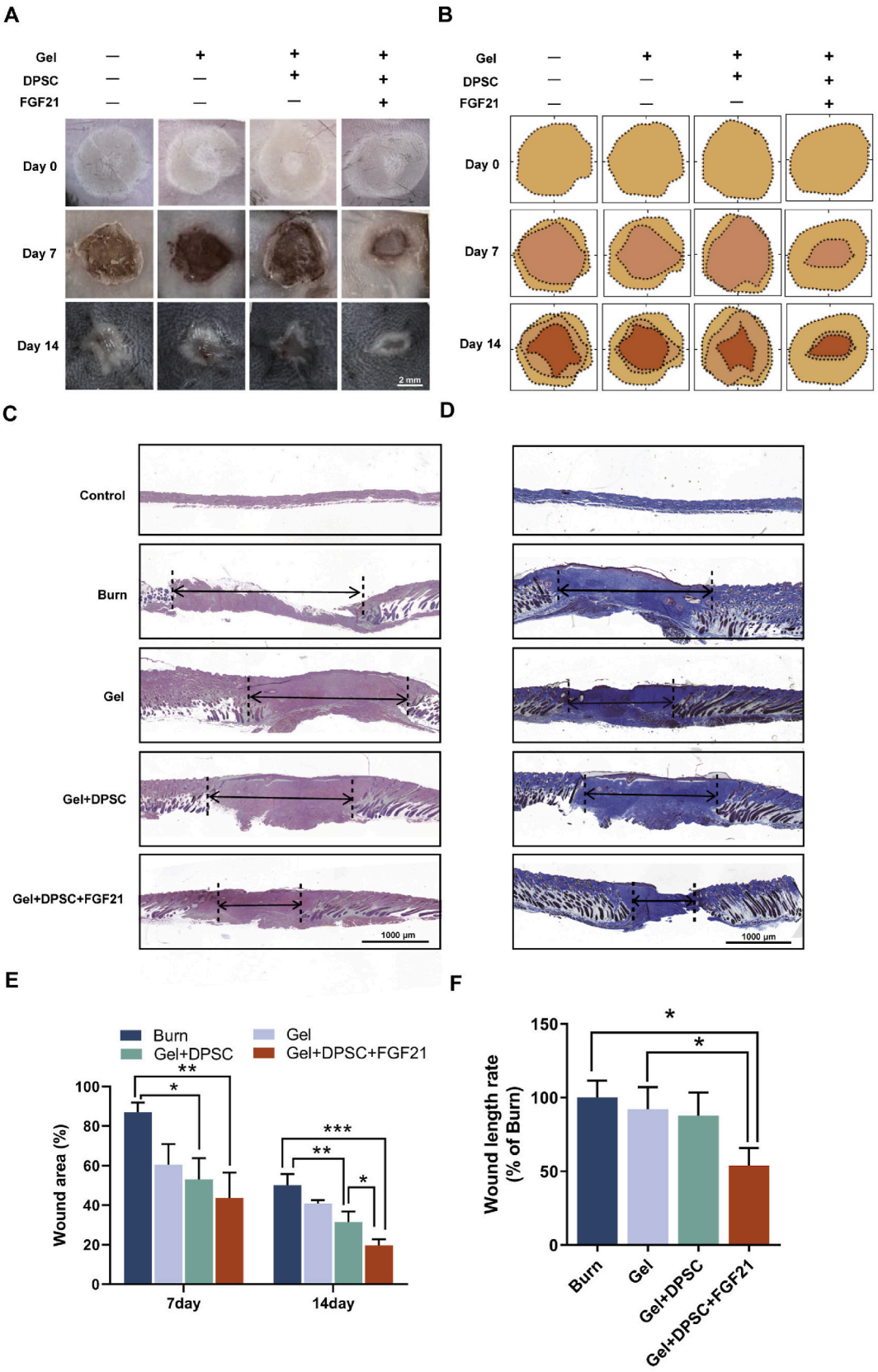

Fig. 4. Wound closure of Gel + DPSC + FGF21 treatment in diabetic mice. (A) Photographs of four types of treated wounds on day 0, 7, 14. Scale: 2 mm. (B) Simulation plots. (C, D) Images of H&E and Masson staining of wound after 14 d of treatments. Scale: 1000 μm. (E) Quantitative analyze of the wound area. (F) Quantitative analysis of the wound length rate. * represents $P < 0.05$. ** represents $P < 0.01$. *** represents $P < 0.001$. Data are represented as mean ± SD (n = 3).

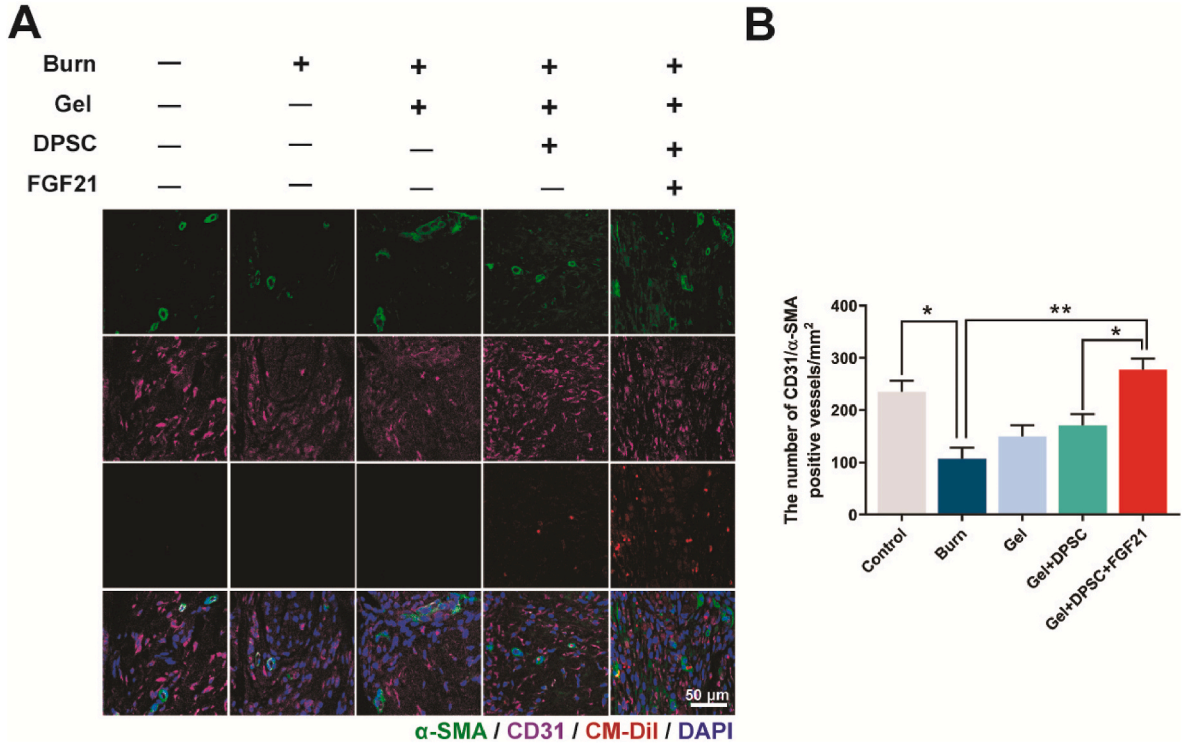

Fig. 5. Cadherin-responsive hydrogel combined with DPSCs and FGF21 promotes the recovery of blood perfusion in diabetic scald skin. (A) Immunofluorescence images of α-SMA (green), CD31 (purple), CM-Dil (red) and DAPI (blue) in the indicated groups. Scale: 50 μm. (B) Morphometric analysis of new and mature blood vessels. * represents $P < 0.05$. ** represents $P < 0.01$. Data are represented as mean ± SD (n = 3). PECAM-1/CD31: Platelet endothelial cell adhesion molecule-1; α-SMA: α-smooth muscle actin.

critical importance. Immunofluorescence and WB were used to detect the expression of E cadherin and N cadherin. The results showed that the cadherin-responsive hydrogel was able to recruit cadherin to the epidermis, and FGF21 and DPSCs synergistically promoted the recruitment of cadherin to the epidermis by immunofluorescence staining (Fig. 3A–C). At the same time, the cadherin responsive hydrogel and FGF21 could promote the transition of N cadherin to E cadherin by WB analyses (Fig. 3D–F). In summary, cadherin-responsive hydrogel combined with DPSCs and FGF21 achieved rapid epithelial recovery via the regulation of EMT as evidenced by cadherin switching.

3.4. Cadherin-responsive hydrogel combined with DPSCs and FGF21 promotes scald repair in diabetic mice

Diabetic scald is a common refractory wound. Due to the microenvironment of high glucose and high oxidation, and the decrease in blood perfusion, the repair of skin has significantly slowed down [36]. To verify whether the cadherin-responsive hydrogel combined with DPSCs and FGF21 could promote the repair of diabetic scald wounds, we recorded the wound recovery of scalded diabetic mice on day 0, 7, and 14. The results showed that in the high glucose state, blood vessels and subcutaneous fat were reduced, so the skin was thinner than normal skin [37]. Notably, the cadherin-responsive hydrogel combined with DPSCs and FGF21 could also effectively promote the repair of diabetic wounds (Fig. 4A–B, E). The results of H&E staining and Masson staining showed that the repair effect of hydrogel on diabetic scald wounds was weaker than that of normal control mice. There was no significant hair follicle regeneration in the injured center, but the injured area was significantly reduced, collagen deposition was increased, and hair follicle regeneration was also observed at the edge of the injured area (Fig. 4C–D, F).

Next, we used the immunofluorescence to detect the expression of the blood vessels, the experimental results showed that in diabetic mice, scalded wounds further reduced blood vessels, cadherin-responsive hydrogel could not protect scald caused by vascular damage. Interestingly, after adding DPSCs, hydrogel could effectively promote the vascular regeneration of diabetic scald wound, indicating that DPSCs have vascular differentiation ability. However, the blood vessels formed were mainly neovascularization. Remarkably, after the addition of FGF21, the ability of hydrogel to promote vascular maturation was greatly enhanced with increased $CD31^+$ endothelial cells associated with αSMA^+ cell, which was predicted to be beneficial to the recovery of blood perfusion in diabetic scald skin. We also found a partial colocalization of $CD31^+$ and $CMDil^+$ cells in the Gel + DPSC + FGF21 group (Fig. 5A and B).

We conducted weekly monitoring of the mice's weight and random blood glucose levels throughout the duration of the study. Notably, at the conclusion of the experiment, it was observed that both Gel + DPSC and Gel + DPSC + FGF21 groups exhibited lower blood glucose levels compared to the Burn group (Sfig 3A-C). Furthermore, on days 7 and 14, both experimental groups demonstrated a greater increase in body weight when compared to the Burn group (Sfig 3D-F), indicating that the combination of cadherin-responsive hydrogels with DPSC and FGF21 improved basal metabolism in diabetic mice. In conclusion, cadherin-responsive hydrogel combined with DPSCs and FGF21 could effectively promote the recovery of diabetic scald.

3.5. Cadherin-responsive hydrogel combined with DPSCs and FGF21 regulates epithelial EMT in diabetic scald

Immunofluorescence results showed that diabetic skin had a high expression of N-cadherin and a low expression of E-cadherin. After treatment, the high expression of E-cadherin in diabetic scald epithelium was promoted to accelerate epithelial recovery through the cadherin recruitment effect of cadherin-responsive hydrogel with the cadherin switching of N cadherin to E cadherin, indicating that EMT has taken place (Fig. 6A, C). The immunofluorescence results showed that the

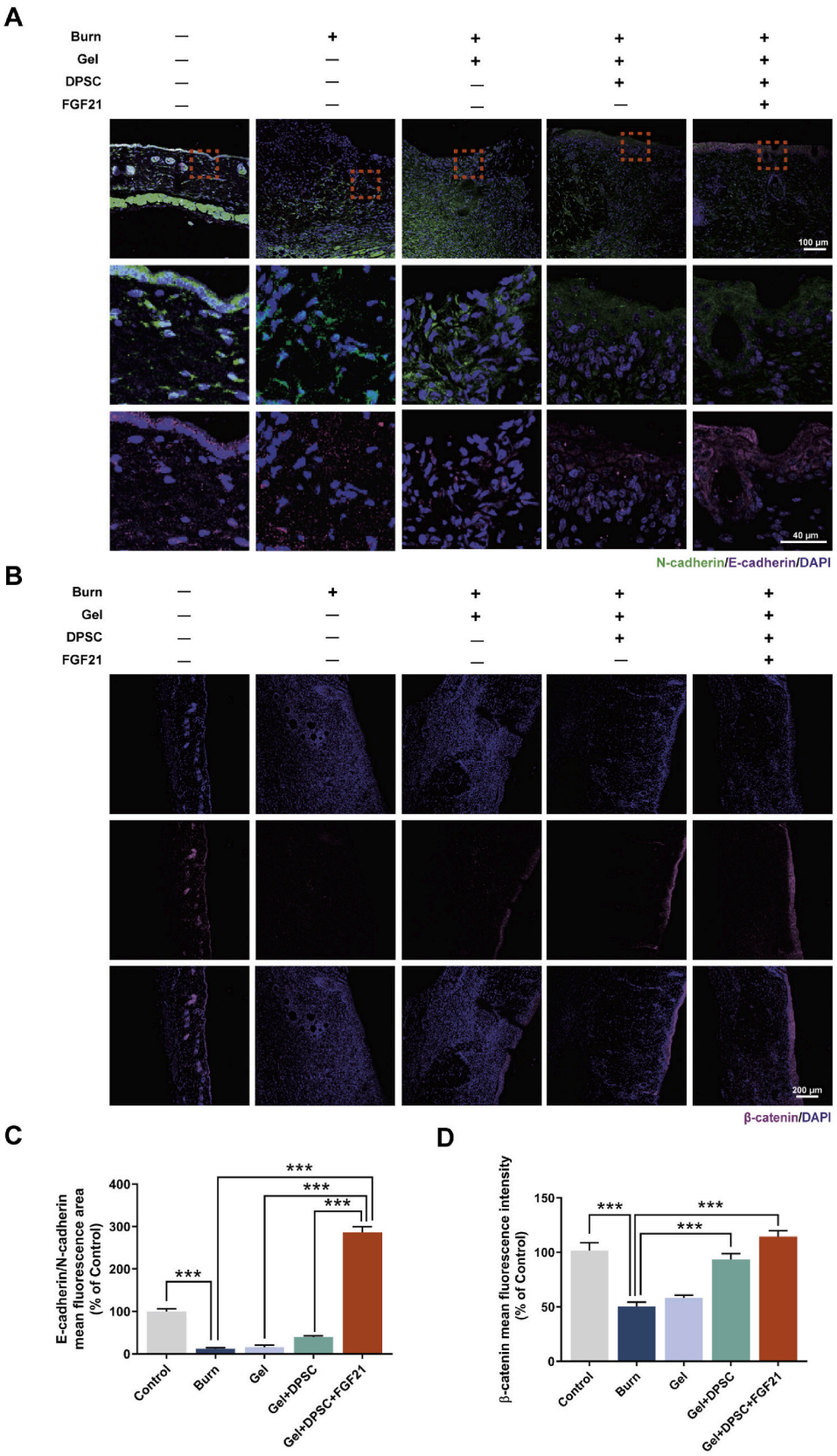

Fig. 6. Cadherin-responsive hydrogel combined with DPSCs and FGF21 promotes the transition of N cadherin to E cadherin in diabetic mice. (A) Immunofluorescence showing the expression of N-cadherin (green) and E-cadherin (purple) in different groups at day 14. The nuclear is labeled by DAPI (blue). Scale: 100 μm. A boxed region illustrates a representative region with high power images, scale: 40 μm. (B) Immunofluorescence showing the expression of β-catenin (purple) in different groups at day 14. The nuclear is labeled by DAPI (blue). Scale: 200 μm. (C) Mean fluorescence area of E-cadherin/N-cadherin in the indicated groups. (D) Mean fluorescence intensity of β-catenin in the indicated groups. *** represents $P < 0.001$. Data are represented as mean ± SD ($n = 3$).

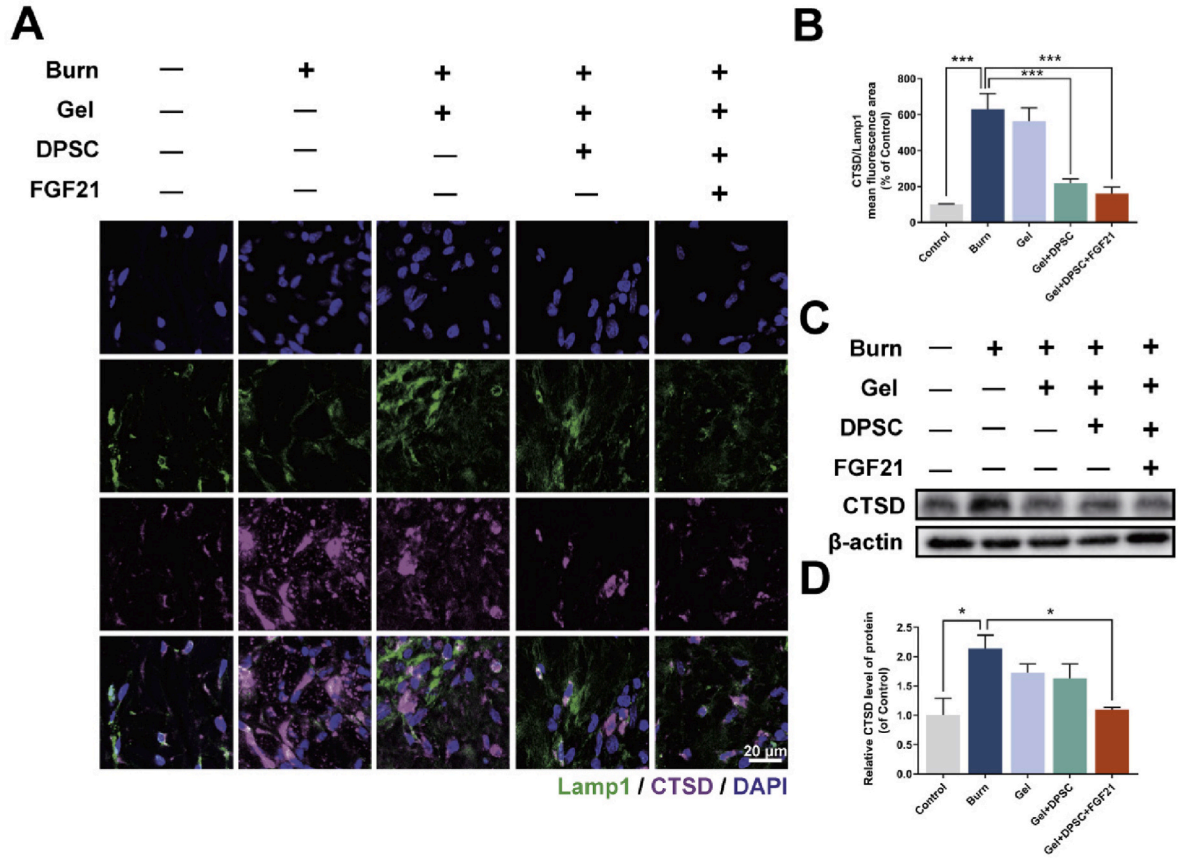

Fig. 7. Lysosomal hyperfunction is significantly improved after the treatment of cadherin-responsive hydrogel combined with DPSCs and FGF21 in diabetic mice. (A) Immunofluorescence showing the expression of Lamp (green) and CTSD (purple) in different groups at day 14. The nuclear is labeled by DAPI (blue). Scale: 20 μm. (B) Mean fluorescence area of CTSD/Lamp1 in the indicated groups. (C, D) Representative images and analysis of western blots of CTSD in the indicated groups. β-actin was used as a reference. * represents $P < 0.05$. *** represents $P < 0.001$. Data are represented as mean ± SD (n = 3). LAMP1: lysosomal-associated membrane protein 1; CTSD: cathepsin D.

hydrogel could effectively up-regulate the expression of β-Catenin, an important protein that promotes the transition from N cadherin to E cadherin, indicative of the regulatory effect of hydrogel on EMT (Fig. 6B, D). In conclusion, cadherin-responsive hydrogel combined with DPSCs and FGF21 could effectively promote EMT as evidenced by the transition of N cadherin to E cadherin accompanied with increased expression of β-Catenin in diabetic scald model.

3.6. Cadherin-responsive hydrogel combined with DPSCs and FGF21 improves the survival of diabetic scald skin cells

Reactive oxygen species (ROS) produced in diabetic conditions can affect the function of membrane organelles to varying degrees, and the high temperature of scald can further damage membrane organelles in cells [38]. Our results demonstrated that the expression of lysosomal aspartic protease cathepsin D (CTSD) was increased after scald, and treatment of cadherin-responsive hydrogel combined with DPSCs and FGF21 inhibited the expression of CTSD by confocal microscopy analyses (Fig. 7A and B) and Western blot assays (Fig. 7C and D), and this effect was mainly achieved by FGF21. In addition, cadherin-responsive hydrogel combined with DPSCs and FGF21 also led to re-encapsulated by lysosomes as evidenced by colocalization of CTSD and Lamp1 by confocal microscopy analyses (Fig. 7A and B). Our cell experiments also confirmed that FGF21 effectively alleviated the lysosomal hyperfunction induced by ROS under high glucose condition (Sfig 4A-C). Then we tested the indicators of necroptosis to confirm the survival status of scalded epidermis. The results showed that in cadherin-responsive hydrogel combined with DPSCs and FGF21 system, FGF21 played the most important role in the treatment of the scalded epidermis, and the necroptosis marker, p-MLKL expression was significantly inhibited (Sfig 5A, B). Autophagy is a key pathway for cells to resist external stress and improve cell survival rate. The role of lysosomes is closely related to autophagy [39,40]. The results showed that after the improvement of lysosomal stability with an increased expression of C-CASP8 by hydrogel treatment (Sfig 5C, D), autophagy was activated in scald epithelium as evidenced with an increased expression of LC3B and a decreased expression of p62 (Sfig 6A-C). Taken together, these results suggest that cadherin-responsive hydrogel combined with DPSCs and FGF21 attenuated necroptosis in diabetic scald by improving lysosomal stability and activating autophagy.

3.7. Cadherin-responsive hydrogel combined with DPSCs and FGF21 improves autophagic flux and inhibits necroptosis by regulating lysosomal stability

To further test whether hydrogel could inhibit necroptosis by activating autophagy through regulating lysosomal stability, we used lysosomal membrane detergent NDI and cellular phospholipase A2 inhibitor CAY10650. The experimental results showed that NDI could effectively destroy the lysosomal membrane, accompanied by releasing a large amount of hydrolase to cytosol, whereas cadherin-responsive hydrogel combined with DPSCs and FGF21 treatment stabilized the lysosomes as evidenced by the decreased expression of CTSD by confocal microscopy analyses (Fig. 8A and B) and Western blot assays (Fig. 8C and D). In addition, after the inhibition of cellular phospholipase A2 by CAY10650, the destruction of lysosomal membrane was inhibited, and the hydrolase

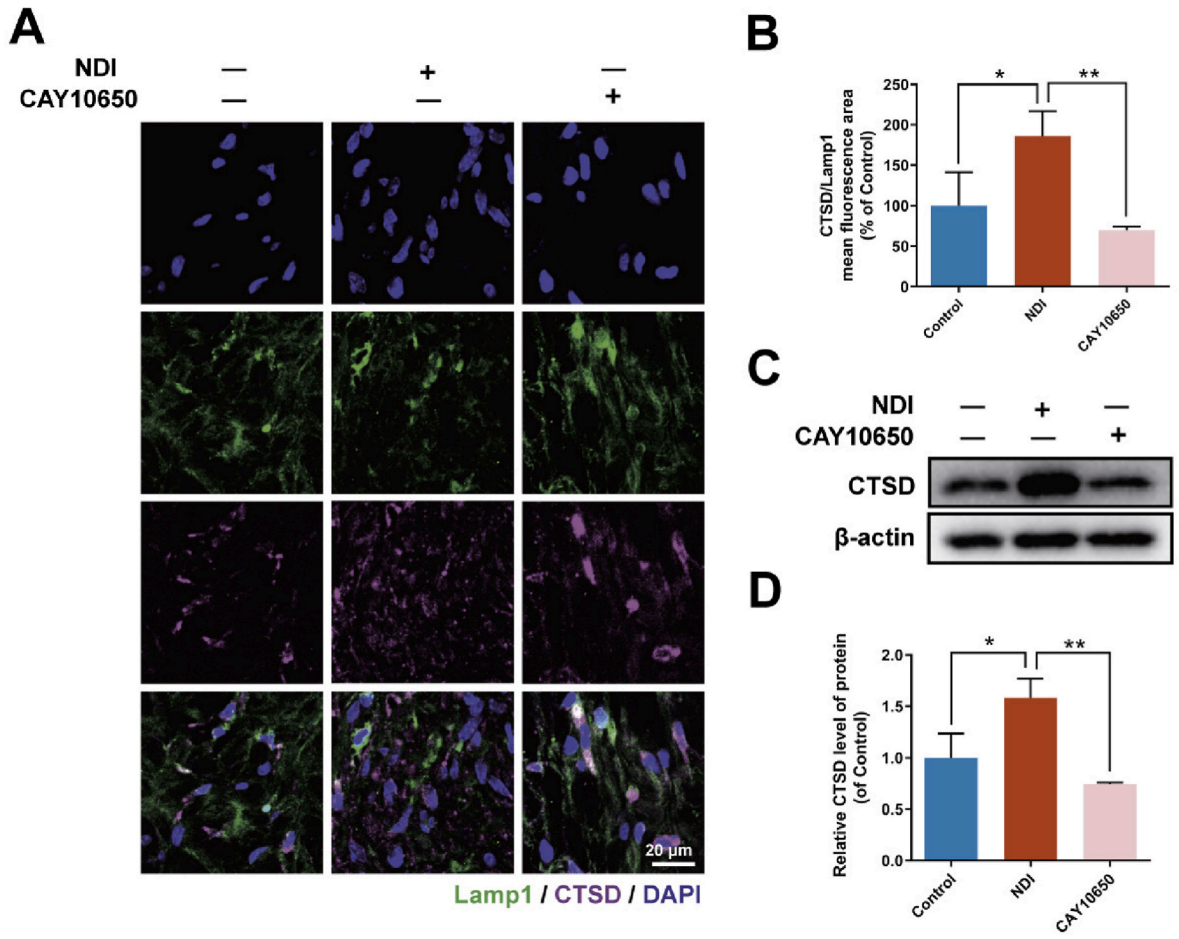

Fig. 8. Cadherin-responsive hydrogel combined with DPSCs and FGF21 inhibits necroptosis by regulating lysosomal stability in diabetic mice. (A) Immunofluorescence showing the expression of Lamp1 (green) and CTSD (purple) in different groups. The nuclear is labeled by DAPI (blue). Scale: 20 μm. (B) Mean fluorescence area of CTSD/Lamp1 in the indicated groups. (C, D) Representative images and analysis of Western blots of CTSD in the indicated groups. β-actin was used as a reference. * represents $P < 0.05$. ** represents $P < 0.01$. Data are represented as mean ± SD (n = 3). LAMP1: lysosomal-associated membrane protein 1; CTSD: cathepsin D.

was re-encapsulated by lysosomes (Fig. 8A and B).

At the same time, the apparent repair of the skin was also measured. The results showed that NDI could significantly aggravate scald injury, whereas CAY10650 could cooperate with the cadherin-responsive hydrogel combined with DPSCs and FGF21 to accelerate recovery. The visual recovery images of the tissue showed that after 14 days of repair, the damaged area after NDI treatment was significantly larger than that of the control treatment group, and the damaged area could be repaired after CAY10650 which was involved in maintaining the stability of lysosomes (Fig. 9A–B, E). The results of H&E and Masson staining showed that the repair rate of diabetic scald significantly slowed down after the stability of lysosomes was compromised, while the maintenance of lysosomal stability could accelerate the repair process (Fig. 9C–D, F).

The results of vascular detection showed that NDI destroyed the stability of lysosomes and significantly inhibited the transformation of neovascularization into mature blood vessels and the stability of blood flow channels. The transformation of neovascularization into mature blood vessels with an increased $CD31^+$ endothelial cells associated with α-SMA^+ cell was restored after the inhibition of cellular phospholipase A2 by CAY10650 (Fig. 10A and B).

We monitored the mice's weight and random blood glucose levels weekly throughout the study period. It is worth noting that on day 7 of the experiment, the NDI group showed higher blood glucose levels than the other two groups, and on day 14, the CAY10650 group showed lower blood glucose levels than the other two groups (Sfig 7A-C). In addition, on day 14, the NDI group exhibited lower body weight than the other two groups (Sfig 7D-F), suggesting that CAY10650 enhanced lysosomal membrane stability was beneficial for improving metabolic levels in diabetic mice.

Next, we also measured the EMT level of the tissue. The results showed that the transition from N cadherin to E cadherin was significantly inhibited and the expression level of β-Catenin was significantly down-regulated after the disruption of lysosome stability. When CAY10650 was added, the conversion efficiency of N cadherin to E cadherin was significantly improved (Fig. 11A. B), and the expression of β-Catenin was also significantly increased (Fig. 11C and D). Finally, we tested the skin tissue necroptosis and autophagy level. The experimental results showed that NDI impaired lysosome stability and activated necroptosis, whereas autophagy was significantly inhibited. After lysosomal stability was restored by CAY10650, necroptosis was inhibited (Sfig 8A-D), and autophagy was reactivated as evidenced with an increased expression of LC3B and a decreased expression of p62 (Sfig 9A-C).

To mimic the pathophysiological process of normal diabetic burn, based on the lysosomal hyperfunction in diabetic burn mice (untreated), we further verified that CAY10650 reduced wound area (Sfig 10A-C), accelerated repair process (Sfig 10D-F) and inhibited necroptosis (Sfig 10G-I) by enhancing lysosomal membrane stability. Taken together, these results suggest that cadherin-responsive hydrogel combined with DPSCs and FGF21 could inhibit necroptosis in diabetic scald by enhancing lysosomal stability and activating autophagic flux.

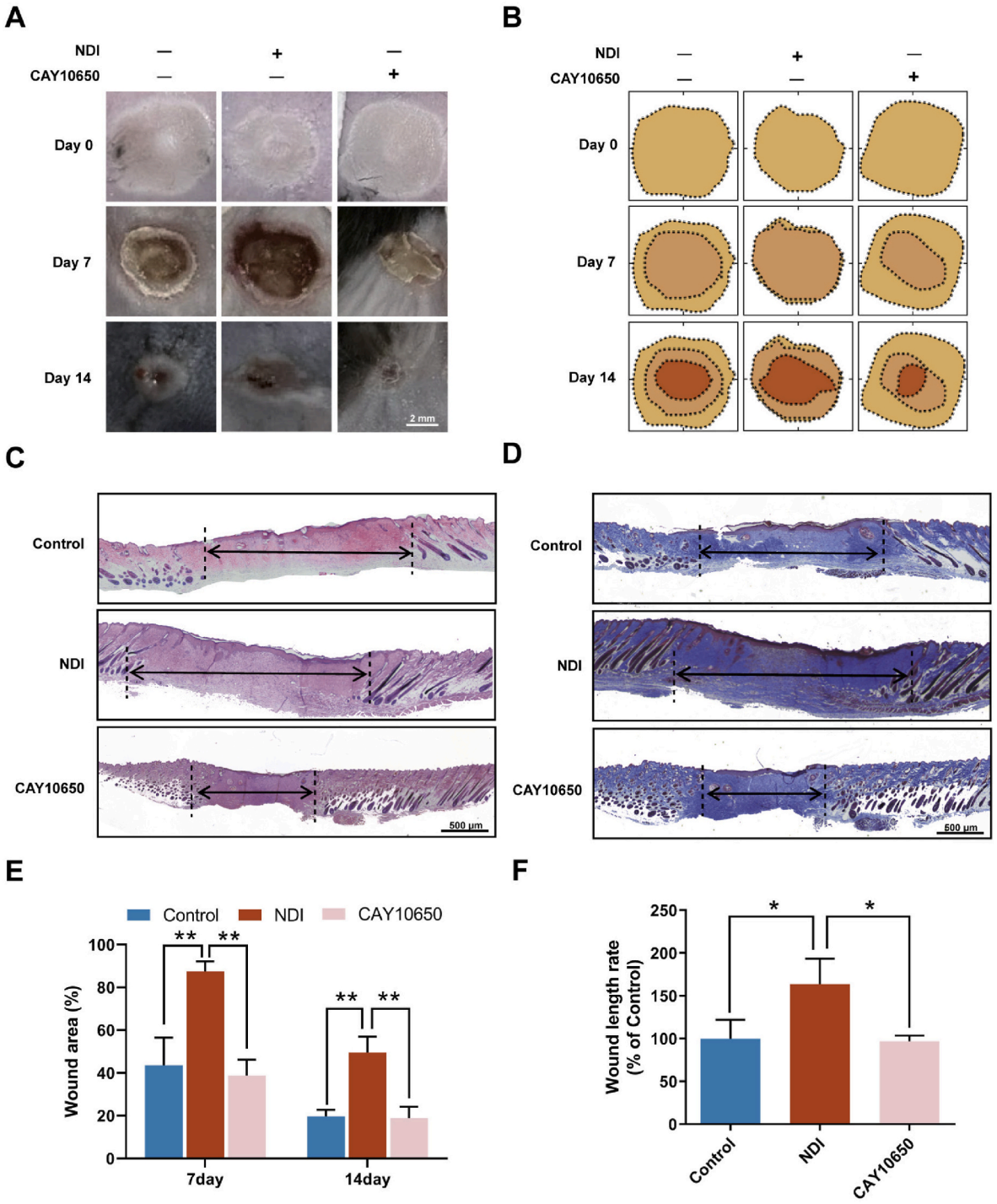

Fig. 9. Maintaining the stability of lysosomes promotes the apparent repair of tissue in diabetic mice with the hydrogel containing FGF21 and DPSCs. (A) Photographs of wounds in the indicated groups on day 0, 7, 14. Scale: 2 mm. (B) Simulation plots. (C, D) Images of H&E and Masson staining of wound after 14 d. Scale: 1000 μm. (E) Quantitative analyze of the wound area. (F) Quantitative analysis of the wound length rate. * represents $P < 0.05$. ** represents $P < 0.01$. Data are represented as mean ± SD (n = 3).

4. Discussion

Due to the high glucose and high oxidation microenvironment, diabetic conditions can lead to slowed cell proliferation, reduced blood perfusion, and impaired epithelial formation [41]. Aiming at these key points of repair, we designed a cadherin-responsive hydrogel combined with DPSCs and FGF21 to recruit cadherins to promote epithelial repair with the hydrogel, promote angiogenesis with DPSCs, and regulate the microenvironment with FGF21 to maintain lysosome stability to achieve comprehensive repair of diabetic scald.

Calcium alginate hydrogel has been widely used in food processing and biomedicine [42,43]. Due to its excellent biological affinity, it often acts as a drug carrier, but the effect of its own action has not been explored [44]. In this study, we propose that it exhibits cadherin-responsive characteristics. Our previous study demonstrated that alginate calcium hydrogel is a cadherin-responsive hydrogel, which can recruit cadherins to the epidermis and regulate EMT through the intracellular calcium ions, which is beneficial for epithelial repair [17].

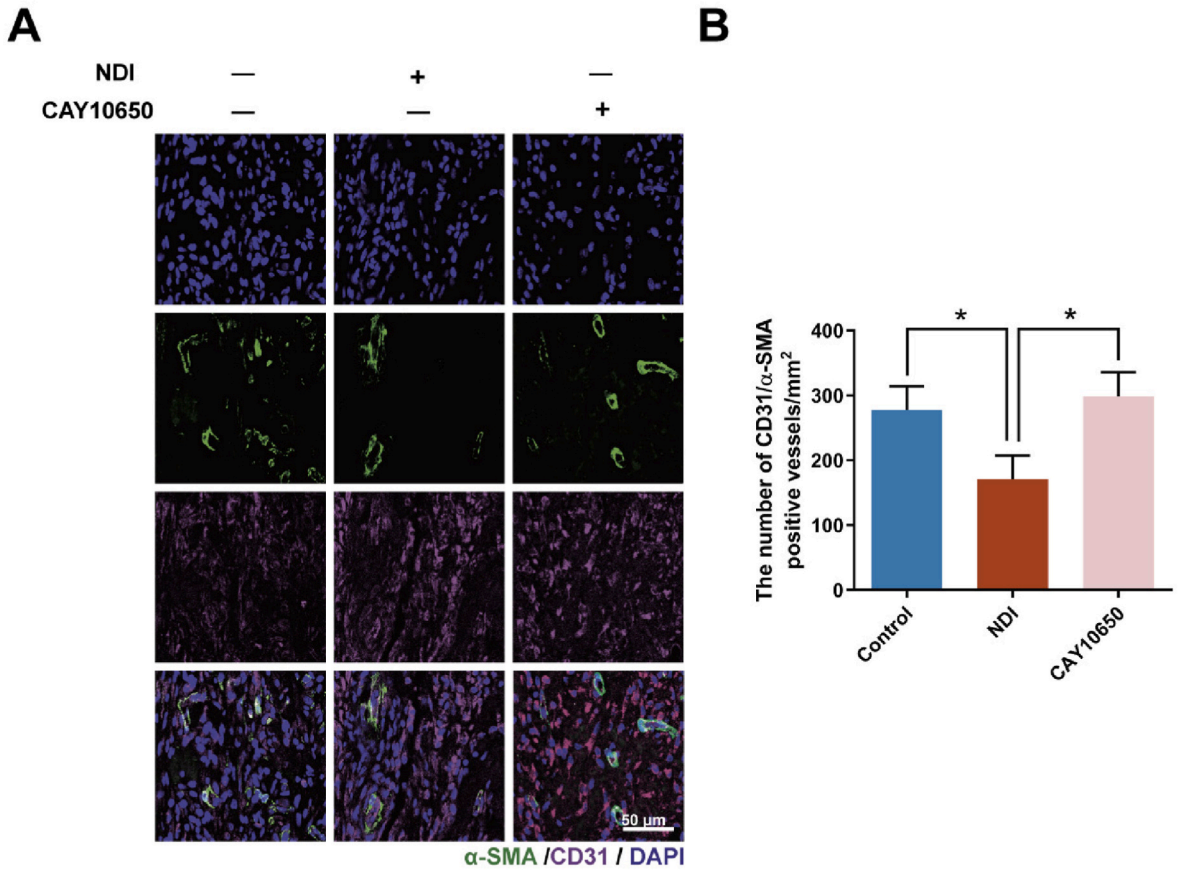

Fig. 10. Restoration of lysosomal stability promotes the recovery of blood perfusion in diabetic mice with the hydrogel containing FGF21 and DPSCs. (A) Immunofluorescence images of α-SMA (green), CD31 (purple), and DAPI (blue) in the indicated groups. Scale: 50 μm. (B) Morphometric analysis of new and mature blood vessels. * represents $P < 0.05$. Data are represented as mean ± SD (n = 3). PECAM-1/CD31: Platelet endothelial cell adhesion molecule-1; α-SMA: α-smooth muscle actin.

At the same time, calcium ions are locked in the hydrogel without causing calcium overload to the tissue, which further improves the biosafety [45]. The expression of N cadherin was significantly up-regulated in diabetic conditions, and EMT showed a transition trend from E cadherin to N cadherin [46]. Our results showed that after scald, the expression of total cadherin was significantly down-regulated in the epithelial layer but N cadherin was highly expressed in the dermal layer. Therefore, a core of treatment strategy was to recruit N cadherin from the dermal layer to the upper layer and convert it to E cadherin. We found that cadherin-responsive hydrogels successfully achieved cadherin recruitment but were not effective in promoting the transition from N cadherin to E cadherin, so additional agents were needed to promote the transition.

FGF21 is a glucose-lipid metabolism regulatory protein, which can effectively regulate the metabolism of cells in diabetic conditions [47,48]. Lin et al. [49] confirmed that FGF21 could effectively up-regulate E cadherin, and the efficiency of promoting N cadherin to E cadherin was significantly improved after adding FGF21 to the hydrogel in our previous study. We also examined the protective effect of the hydrogel on diabetic scald wounds and found that the cell survival status was significantly improved with the addition of FGF21. The high ROS microenvironment in diabetic conditions could make intracellular membrane organelles more vulnerable to damage [50]. Our previous results showed that there was significant lysosomal hyperfunction after diabetic scald, and a large number of hydrolases were released into the cell body, leading to autophagy inhibition and necroptosis. Furthermore, lysosomal membrane detergent NDI and phospholipase A2 inhibitor CAY10650 were used to verify that the protective effect of cadherin-responsive hydrogel combined with DPSCs and FGF21 on tissue cells could be achieved by stabilizing lysosomes.

How to improve tissue blood perfusion after achieving epithelial repair and maintaining cell stability is also the key to promote diabetic scald wound healing [51]. The skin of diabetic patients is often accompanied by a decrease in blood perfusion, which is an important factor for the difficulty of diabetic wound healing [52]. In addition, the microenvironment of high glucose and high oxidation also greatly limits angiogenesis [53]. FGF21 was found to reduce glucose level in the skin wound but appeared to have lack of satisfactory effect on angiogenesis. Accordingly, DPSCs were introduced to further promote angiogenesis. DPSCs have multipotent differentiation properties and can differentiate into vascular endothelial cells [54]. After improving cell stability and glucose tolerance by FGF21, DPSCs could differentiate rapidly to form blood vessels, which could improve tissue blood perfusion, as well as the survival and proliferation of cells in diabetic scald wounds. Notably, DPSCs have low immune rejection properties suitable for allogeneic transplantation and have abundant sources with a very broad potential application in the field of regeneration and repair [55].

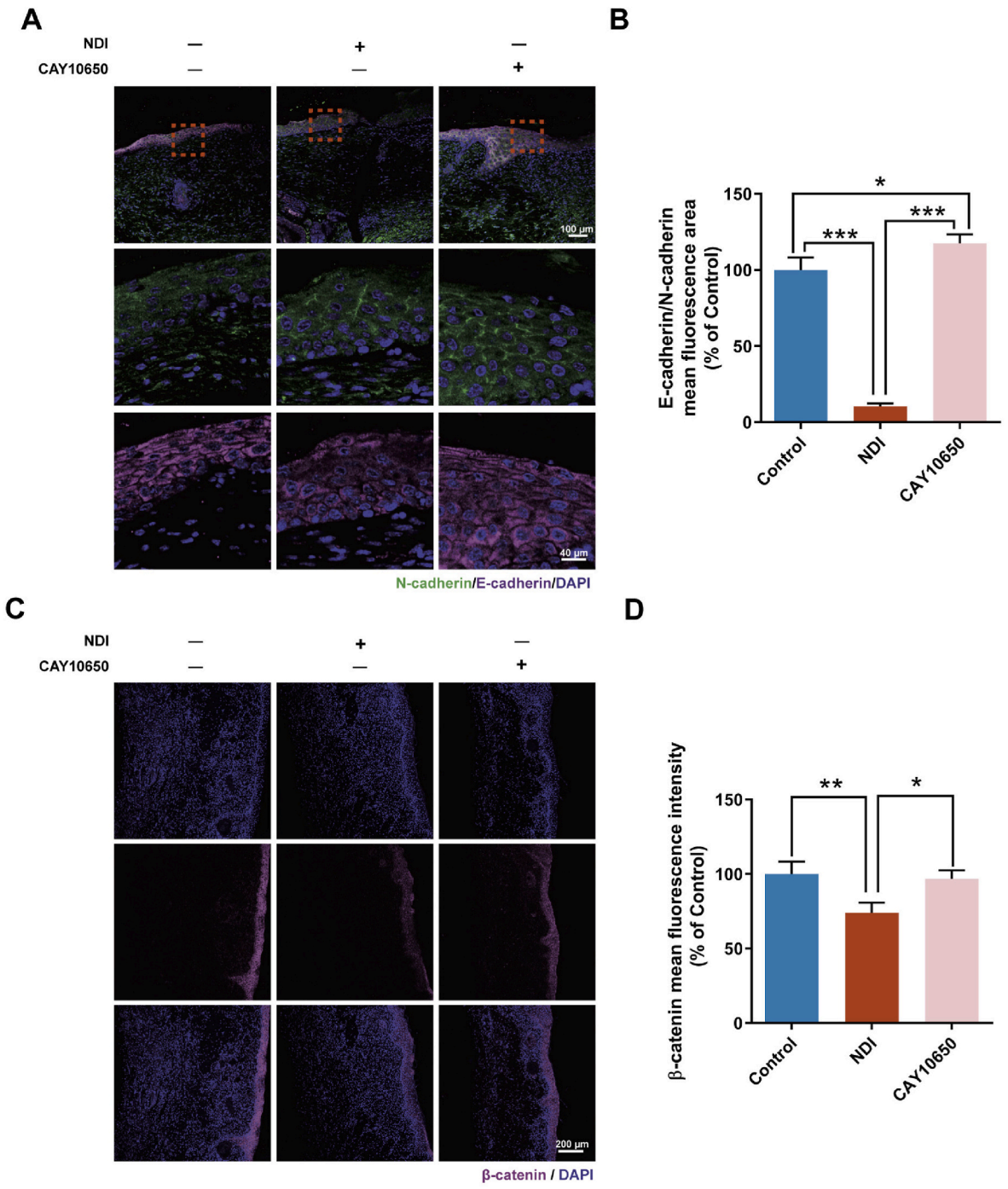

Fig. 11. Maintenance of lysosomal function promotes the transition of N cadherin to E cadherin in diabetic mice with the hydrogel containing FGF21 and DPSCs. (A) Immunofluorescence showing the expression of N-cadherin (green) and E-cadherin (purple) in the indicated groups. The nuclear is labeled by DAPI (blue). Scale: 100 μm. A boxed region illustrates a representative region with high power images, scale: 40 μm. (B) Mean fluorescence area of E-cadherin/N-cadherin in the indicated groups. (C) Immunofluorescence showing the expression of β-catenin (purple) in the indicated groups. The nuclear is labeled by DAPI (blue). Scale: 200 μm. (D) Mean fluorescence intensity of β-catenin in the indicated groups. * represents $P < 0.05$. ** represents $P < 0.01$. *** represents $P < 0.001$. Data are represented as mean ± SD (n = 3).

5. Conclusions

In summary, we have designed a cadherin-responsive hydrogel combined with DPSCs and FGF21 that can simultaneously promote diabetic burn wound healing by 1) promoting cadherin recruitment and the transformation of N cadherin to E cadherin, 2) promoting tissue blood perfusion, and 3) alleviating necroptosis via maintaining lysosomal stability and activating autophagy to improve intracellular homeostasis. These three core functions could simultaneously facilitate the repair of diabetic scald wounds.

Ethics approval and consent to participate

All protocols and animal experiments were conducted in strict accordance with the Animal Care and Use Committee of Wenzhou Medical University (No. WYDW-2018- 0342). All protocols of collection

and application of human dental pulp stem cells were approved by ethical committee of Wenzhou Medical University (No. WYKQ2018008SC).

CRediT authorship contribution statement

Wenjie Lu: Writing - original draft. **Juan Zhao:** Formal analysis, Data curation. **Xiong Cai:** Formal analysis, Data curation. **Yutian Wang:** Methodology, Formal analysis. **Wenwei Lin:** Methodology, Formal analysis. **Yaoping Fang:** Formal analysis. **Yunyang Wang:** Formal analysis. **Jinglei Ao:** Formal analysis. **Jiahui Shou:** Formal analysis. **Jiake Xu:** Writing - review & editing, Supervision, Conceptualization. **Sipin Zhu:** Writing - original draft.

Declaration of competing interest

The authors declare that they have no known competing financial interests or personal relationships that could have appeared to influence the work reported in this paper.

Data availability

Data will be made available on request.

Acknowledgements

This study was partly funded by grants from the National Natural Science Funding of China (82172424, 82372396), Outstanding Youth Fund of Zhejiang Province (LR22H060002), Zhejiang Medical and Health Science and Technology Plan Project (2022RC210), Shenzhen Medical Research Funds (B2302005), and Wenzhou Major Science and Technology Innovation Project Approval Project (ZY2022007).

Appendix A. Supplementary data

Supplementary data to this article can be found online at https://doi.org/10.1016/j.mtbio.2023.100919.

References

[1] E. Barnard, H. Li, Shaping of cutaneous function by encounters with commensals, J. Physiol. 595 (2) (2017) 437–450, https://doi.org/10.1113/JP271638.
[2] W. Oualla-Bachiri, A. Fernandez-Gonzalez, M.I. Quinones-Vico, S. Arias-Santiago, From Grafts to human bioengineered vascularized skin substitutes, Int. J. Mol. Sci. 21 (21) (2020), https://doi.org/10.3390/ijms21218197.
[3] A.D. Widgerow, K. King, I. Tocco-Tussardi, D.A. Banyard, R. Chiang, A. Awad, H. Afzel, S. Bhatnager, S. Melkumyan, G. Wirth, G.R. Evans, The burn wound exudate-an under-utilized resource, Burns 41 (1) (2015) 11–17, https://doi.org/10.1016/j.burns.2014.06.002.
[4] B. Zhang, M. Wang, A. Gong, X. Zhang, X. Wu, Y. Zhu, H. Shi, L. Wu, W. Zhu, H. Qian, W. Xu, HucMSC-exosome mediated-Wnt4 signaling is required for cutaneous wound healing, Stem Cell. 33 (7) (2015) 2158–2168, https://doi.org/10.1002/stem.1771.
[5] R. Li, Y. Li, Y. Wu, Y. Zhao, H. Chen, Y. Yuan, K. Xu, H. Zhang, Y. Lu, J. Wang, X. Li, X. Jia, J. Xiao, Heparin-Poloxamer thermosensitive hydrogel loaded with bFGF and NGF enhances peripheral nerve regeneration in diabetic rats, Biomaterials 168 (2018) 24–37, https://doi.org/10.1016/j.biomaterials.2018.03.044.
[6] W.K. Abdelbasset, S.H. Elsayed, G. Nambi, S.A. Tantawy, D.M. Kamel, M.M. Eid, S. A. Moawd, S.F. Alsubaie, Potential efficacy of sensorimotor exercise program on pain, proprioception, mobility, and quality of life in diabetic patients with foot burns: a 12-week randomized control study, Burns 47 (3) (2021) 587–593, https://doi.org/10.1016/j.burns.2020.08.002.
[7] M.L. Usui, J.N. Mansbridge, W.G. Carter, M. Fujita, J.E. Olerud, Keratinocyte migration, proliferation, and differentiation in chronic ulcers from patients with diabetes and normal wounds, J. Histochem. Cytochem. 56 (7) (2008) 687–696, https://doi.org/10.1369/jhc.2008.951194.
[8] K. Gourishetti, R. Keni, P.G. Nayak, S.R. Jitta, N.A. Bhaskaran, L. Kumar, N. Kumar, N. Krishnadas, R.R. Shenoy, Sesamol-loaded PLGA nanosuspension for accelerating wound healing in diabetic foot ulcer in rats, Int. J. Nanomed. 15 (2020) 9265–9282, https://doi.org/10.2147/IJN.S268941.
[9] P. Rastogi, B. Kandasubramanian, Review of alginate-based hydrogel bioprinting for application in tissue engineering, Biofabrication 11 (4) (2019), 042001, https://doi.org/10.1088/1758-5090/ab331e.
[10] M. Il Kim, C.Y. Park, J.M. Seo, K.S. Kang, K.S. Park, J. Kang, K.S. Hong, Y. Choi, S. Y. Lee, J.P. Park, H.G. Park, T.J. Park, In situ biosynthesis of a metal nanoparticle encapsulated in alginate gel for imageable drug-delivery system, ACS Appl. Mater. Interfaces 13 (31) (2021) 36697–36708, https://doi.org/10.1021/acsami.1c02286.
[11] Q.H. Chen, X.H. Tian, J. Fan, H. Tong, Q. Ao, X.H. Wang, An interpenetrating alginate/gelatin network for three-dimensional (3D) cell cultures and organ bioprinting, Molecules 25 (3) (2020), https://doi.org/10.3390/molecules25030756. ARTN756.
[12] K. Jomova, M. Makova, S.Y. Alomar, S.H. Alwasel, E. Nepovimova, K. Kuca, C. J. Rhodes, M. Valko, Essential metals in health and disease, Chem. Biol. Interact. 367 (2022), https://doi.org/10.1016/j.cbi.2022.110173. ARTN110173.
[13] F. Cheng, Y. Shen, P. Mohanasundaram, M. Lindstrom, J. Ivaska, T. Ny, J. E. Eriksson, Vimentin coordinates fibroblast proliferation and keratinocyte differentiation in wound healing via TGF-beta-Slug signaling, Proc Natl Acad Sci U S A 113 (30) (2016) E4320–E4327, https://doi.org/10.1073/pnas.1519197113.
[14] G. Manfioletti, M. Fedele, Epithelial-mesenchymal transition (EMT) 2021, Int. J. Mol. Sci. 23 (10) (2022), https://doi.org/10.3390/ijms23105848.
[15] C.L. Yan, W.A. Grimm, W.L. Garner, L. Qin, T. Travis, N.M. Tan, Y.P. Han, Epithelial to mesenchymal transition in human skin wound healing is induced by tumor necrosis factor-α through bone morphogenic protein-2, Am. J. Pathol. 176 (5) (2010) 2247–2258, https://doi.org/10.2353/ajpath.2010.090048.
[16] S. Sen, P. Basak, B.P. Sinha, P. Maurye, K.K. Jaiswal, P. Das, T.K. Mandal, Anti-inflammatory effect of epidermal growth factor conjugated silk fibroin immobilized polyurethane ameliorates diabetic burn wound healing, Int. J. Biol. Macromol. 143 (2020) 1009–1032, https://doi.org/10.1016/j.ijbiomac.2019.09.219.
[17] S. Zhu, Y. Ying, Q. Wu, Z. Ni, Z. Huang, P. Cai, Y. Tu, W. Ying, J. Ye, R. Zhang, Y. Zhang, M. Chen, Z. Xiang, H. Dou, Q. Huang, X. Li, H. He, J. Xiao, Q. Ye, Z. Wang, Alginate self-adhesive hydrogel combined with dental pulp stem cells and FGF21 repairs hemisection spinal cord injury via apoptosis and autophagy mechanisms, Chem. Eng. J. 426 (2021), https://doi.org/10.1016/j.cej.2021.130827.
[18] M. Zhao, S. Wang, A. Zuo, J. Zhang, W. Wen, W. Jiang, H. Chen, D. Liang, J. Sun, M. Wang, HIF-1alpha/JMJD1A signaling regulates inflammation and oxidative stress following hyperglycemia and hypoxia-induced vascular cell injury, Cell. Mol. Biol. Lett. 26 (1) (2021) 40, https://doi.org/10.1186/s11658-021-00283-8.
[19] P.F. Hsieh, C.C. Yu, P.M. Chu, P.L. Hsieh, Verbascoside protects gingival cells against high glucose-induced oxidative stress via PKC/HMGB1/RAGE/NFkappaB pathway, Antioxidants (Basel) 10 (9) (2021), https://doi.org/10.3390/antiox10091445.
[20] K.L. Ho, Q.G. Karwi, D. Connolly, S. Pherwani, E.B. Ketema, J.R. Ussher, G. D. Lopaschuk, Metabolic, structural and biochemical changes in diabetes and the development of heart failure, Diabetologia 65 (3) (2022) 411–423, https://doi.org/10.1007/s00125-021-05637-7.
[21] B.A. Omar, B. Andersen, J. Hald, K. Raun, E. Nishimura, B. Ahren, Fibroblast growth factor 21 (FGF21) and glucagon-like peptide 1 contribute to diabetes resistance in glucagon receptor-deficient mice, Diabetes 63 (1) (2014) 101–110, https://doi.org/10.2337/db13-0710.
[22] L. Wang, M. Mazagova, C. Pan, S. Yang, K. Brandl, J. Liu, S.M. Reilly, Y. Wang, Z. Miao, R. Loomba, N. Lu, Q. Guo, J. Liu, R.T. Yu, M. Downes, R.M. Evans, D. A. Brenner, A.R. Saltiel, B. Beutler, B. Schnabl, YIPF6 controls sorting of FGF21 into COPII vesicles and promotes obesity, Proc Natl Acad Sci U S A 116 (30) (2019) 15184–15193, https://doi.org/10.1073/pnas.1904360116.
[23] L.D. BonDurant, M. Ameka, M.C. Naber, K.R. Markan, S.O. Idiga, M.R. Acevedo, S. A. Walsh, D.M. Ornitz, M.J. Potthoff, FGF21 regulates metabolism through adipose-dependent and -independent mechanisms, Cell Metabol. 25 (4) (2017) 935–944 e4, https://doi.org/10.1016/j.cmet.2017.03.005.
[24] H. Lu, C. Jia, D. Wu, H. Jin, Z. Lin, J. Pan, X. Li, W. Wang, Fibroblast growth factor 21 (FGF21) alleviates senescence, apoptosis, and extracellular matrix degradation in osteoarthritis via the SIRT1-mTOR signaling pathway, Cell Death Dis. 12 (10) (2021) 865, https://doi.org/10.1038/s41419-021-04157-x.
[25] W. Qiang, T. Shen, M. Noman, J. Guo, Z. Jin, D. Lin, J. Pan, H. Lu, X. Li, F. Gong, Fibroblast growth factor 21 augments autophagy and reduces apoptosis in damaged liver to improve tissue regeneration in zebrafish, Front. Cell Dev. Biol. 9 (2021), 756743, https://doi.org/10.3389/fcell.2021.756743.
[26] Y. Liu, L. Gan, D.X. Cui, S.H. Yu, Y. Pan, L.W. Zheng, M. Wan, Epigenetic regulation of dental pulp stem cells and its potential in regenerative endodontics, World J. Stem Cell. 13 (11) (2021) 1647–1666, https://doi.org/10.4252/wjsc.v13.i11.1647.
[27] S. Zhu, Y. Ying, Y. He, X. Zhong, J. Ye, Z. Huang, M. Chen, Q. Wu, Y. Zhang, Z. Xiang, Y. Tu, W. Ying, J. Xiao, X. Li, Q. Ye, Z. Wang, Hypoxia response element-directed expression of bFGF in dental pulp stem cells improve the hypoxic environment by targeting pericytes in SCI rats, Bioact. Mater. 6 (8) (2021) 2452–2466, https://doi.org/10.1016/j.bioactmat.2021.01.024.
[28] H. Nam, G.H. Kim, Y.K. Bae, D.E. Jeong, K.M. Joo, K. Lee, S.H. Lee, Angiogenic capacity of dental pulp stem cell regulated by SDF-1alpha-CXCR4 Axis, Stem Cell. Int. 2017 (2017), 8085462, https://doi.org/10.1155/2017/8085462.
[29] X. Gao, W. Qin, L. Chen, W. Fan, T. Ma, A. Schneider, M. Yang, O.N. Obianom, J. Chen, M.D. Weir, Y. Shu, L. Zhao, Z. Lin, H.H.K. Xu, Effects of targeted delivery of metformin and dental pulp stem cells on osteogenesis via demineralized dentin matrix under high glucose conditions, ACS Biomater. Sci. Eng. 6 (4) (2020) 2346–2356, https://doi.org/10.1021/acsbiomaterials.0c00124.
[30] E. Zeimaran, S. Pourshahrestani, A. Fathi, N.A.B. Razak, N.A. Kadri, A. Sheikhi, F. Baino, Advances in bioactive glass-containing injectable hydrogel biomaterials

for tissue regeneration, Acta Biomater. 136 (2021) 1–36, https://doi.org/10.1016/j.actbio.2021.09.034.
[31] E. Goleva, E. Berdyshev, D.Y. Leung, Epithelial barrier repair and prevention of allergy, J. Clin. Invest. 129 (4) (2019) 1463–1474, https://doi.org/10.1172/JCI124608.
[32] A. Shpichka, D. Butnaru, E.A. Bezrukov, R.B. Sukhanov, A. Atala, V. Burdukovskii, Y. Zhang, P. Timashev, Skin tissue regeneration for burn injury, Stem Cell Res. Ther. 10 (1) (2019) 94, https://doi.org/10.1186/s13287-019-1203-3.
[33] S.J. Serrano-Gomez, M. Maziveyi, S.K. Alahari, Regulation of epithelial-mesenchymal transition through epigenetic and post-translational modifications, Mol. Cancer 15 (2016) 18, https://doi.org/10.1186/s12943-016-0502-x.
[34] C.Y. Loh, J.Y. Chai, T.F. Tang, W.F. Wong, G. Sethi, M.K. Shanmugam, P.P. Chong, C.Y. Looi, The E-cadherin and N-cadherin switch in epithelial-to-mesenchymal transition: signaling, therapeutic implications, and challenges, Cells 8 (10) (2019), https://doi.org/10.3390/cells8101118.
[35] J. Yang, P. Antin, G. Berx, C. Blanpain, T. Brabletz, M. Bronner, K. Campbell, A. Cano, J. Casanova, G. Christofori, S. Dedhar, R. Derynck, H.L. Ford, J. Fuxe, A. Garcia de Herreros, G.J. Goodall, A.K. Hadjantonakis, R.Y.J. Huang, C. Kalcheim, R. Kalluri, Y. Kang, Y. Khew-Goodall, H. Levine, J. Liu, G. D. Longmore, S.A. Mani, J. Massague, R. Mayor, D. McClay, K.E. Mostov, D. F. Newgreen, M.A. Nieto, A. Puisieux, R. Runyan, P. Savagner, B. Stanger, M. P. Stemmler, Y. Takahashi, M. Takeichi, E. Theveneau, J.P. Thiery, E. W. Thompson, R.A. Weinberg, E.D. Williams, J. Xing, B.P. Zhou, G. Sheng, E.M.T. I. Association, Guidelines and definitions for research on epithelial-mesenchymal transition, Nat. Rev. Mol. Cell Biol. 21 (6) (2020) 341–352, https://doi.org/10.1038/s41580-020-0237-9.
[36] Q. Bai, K. Han, K. Dong, C. Zheng, Y. Zhang, Q. Long, T. Lu, Potential applications of nanomaterials and Technology for diabetic wound healing, Int. J. Nanomed. 15 (2020) 9717–9743, https://doi.org/10.2147/IJN.S276001.
[37] D. Liang, W.J. Lin, M. Ren, J. Qiu, C. Yang, X. Wang, N. Li, T. Zeng, K. Sun, L. You, L. Yan, W. Wang, m(6)A reader YTHDC1 modulates autophagy by targeting SQSTM1 in diabetic skin, Autophagy 18 (6) (2022) 1318–1337, https://doi.org/10.1080/15548627.2021.1974175.
[38] H. Rizwan, S. Pal, S. Sabnam, A. Pal, High glucose augments ROS generation regulates mitochondrial dysfunction and apoptosis via stress signalling cascades in keratinocytes, Life Sci. 241 (2020), 117148, https://doi.org/10.1016/j.lfs.2019.117148.
[39] J. Lou, X. Wang, H. Zhang, G. Yu, J. Ding, X. Zhu, Y. Li, Y. Wu, H. Xu, H. Xu, W. Gao, J. Xiao, K. Zhou, Inhibition of PLA2G4E/cPLA2 promotes survival of random skin flaps by alleviating Lysosomal membrane permeabilization-Induced necroptosis, Autophagy 18 (8) (2022) 1841–1863, https://doi.org/10.1080/15548627.2021.2002109.
[40] C. Sarkar, J.W. Jones, N. Hegdekar, J.A. Thayer, A. Kumar, A.I. Faden, M.A. Kane, M.M. Lipinski, PLA2G4A/cPLA2-mediated lysosomal membrane damage leads to inhibition of autophagy and neurodegeneration after brain trauma, Autophagy 16 (3) (2020) 466–485, https://doi.org/10.1080/15548627.2019.1628538.
[41] S.R.U. Rehman, R. Augustine, A.A. Zahid, R. Ahmed, M. Tariq, A. Hasan, Reduced graphene oxide incorporated GelMA hydrogel promotes angiogenesis for wound healing applications, Int. J. Nanomed. 14 (2019) 9603–9617, https://doi.org/10.2147/IJN.S218120.
[42] H. Zhang, J. Cheng, Q. Ao, Preparation of alginate-based biomaterials and their applications in biomedicine, Mar. Drugs 19 (5) (2021), https://doi.org/10.3390/md19050264.
[43] A. Hurtado, A.A.A. Aljabali, V. Mishra, M.M. Tambuwala, A. Serrano-Aroca, Alginate: enhancement strategies for advanced applications, Int. J. Mol. Sci. 23 (9) (2022), https://doi.org/10.3390/ijms23094486.
[44] N.M. Sanchez-Ballester, I. Soulairol, B. Bataille, T. Sharkawi, Flexible heteroionic calcium-magnesium alginate beads for controlled drug release, Carbohydr. Polym. 207 (2019) 224–229, https://doi.org/10.1016/j.carbpol.2018.11.096.
[45] G.G. Chen, Y.X. Zhou, J. Dai, S.Y. Yan, W.J. Miao, L.L. Ren, Calcium alginate/PNIPAAm hydrogel with body temperature response and great biocompatibility: application as burn wound dressing, Int. J. Biol. Macromol. 216 (2022) 686–697, https://doi.org/10.1016/j.ijbiomac.2022.07.019.
[46] T.T. Wu, Y.Y. Chen, H.Y. Chang, Y.H. Kung, C.J. Tseng, P.W. Cheng, AKR1B1-Induced epithelial-mesenchymal transition mediated by RAGE-oxidative stress in diabetic cataract lens, Antioxidants (Basel) 9 (4) (2020), https://doi.org/10.3390/antiox9040273.
[47] J. Yan, Y. Nie, J. Cao, M. Luo, M. Yan, Z. Chen, B. He, The roles and pharmacological effects of FGF21 in preventing aging-associated metabolic diseases, Front Cardiovasc Med 8 (2021), 655575, https://doi.org/10.3389/fcvm.2021.655575.
[48] X. Yang, R. Yang, M. Chen, Q. Zhou, Y. Zheng, C. Lu, J. Bi, W. Sun, T. Huang, L. Li, J. Gong, X. Li, Q. Hui, X. Wang, KGF-2 and FGF-21 poloxamer 407 hydrogel coordinates inflammation and proliferation homeostasis to enhance wound repair of scalded skin in diabetic rats, BMJ Open Diabetes Res Care 8 (1) (2020), https://doi.org/10.1136/bmjdrc-2019-001009.
[49] S. Lin, L. Yu, Y. Ni, L. He, X. Weng, X. Lu, C. Zhang, Fibroblast growth factor 21 attenuates diabetes-induced renal fibrosis by negatively regulating TGF-beta-p53-smad2/3-mediated epithelial-to-mesenchymal transition via activation of AKT, Diabetes Metab. J 44 (1) (2020) 158–172, https://doi.org/10.4093/dmj.2018.0235.
[50] F. Paneni, J.A. Beckman, M.A. Creager, F. Cosentino, Diabetes and vascular disease: pathophysiology, clinical consequences, and medical therapy: part I, Eur. Heart J. 34 (31) (2013) 2436–2443, https://doi.org/10.1093/eurheartj/eht149.
[51] U.A. Okonkwo, L.A. DiPietro, Diabetes and wound angiogenesis, Int. J. Mol. Sci. 18 (7) (2017), https://doi.org/10.3390/ijms18071419.
[52] J. Yang, Z. Chen, D. Pan, H. Li, J. Shen, Umbilical cord-derived mesenchymal stem cell-derived exosomes combined pluronic F127 hydrogel promote chronic diabetic wound healing and complete skin regeneration, Int. J. Nanomed. 15 (2020) 5911–5926, https://doi.org/10.2147/IJN.S249129.
[53] Q.Y. Ding, T.F. Sun, W.J. Su, X.R. Jing, B. Ye, Y.L. Su, L. Zeng, Y.Z. Qu, X. Yang, Y. Z. Wu, Z.Q. Luo, X.D. Guo, Bioinspired multifunctional black phosphorus hydrogel with antibacterial and antioxidant properties: a stepwise countermeasure for diabetic skin wound healing, Adv. Healthcare Mater. 11 (12) (2022), https://doi.org/10.1002/adhm.202102791. ARTN2102791.
[54] Z. Zhang, M. Oh, J.I. Sasaki, J.E. Nor, Inverse and reciprocal regulation of p53/p21 and Bmi-1 modulates vasculogenic differentiation of dental pulp stem cells, Cell Death Dis. 12 (7) (2021) 644, https://doi.org/10.1038/s41419-021-03925-z.
[55] B. Sui, D. Wu, L. Xiang, Y. Fu, X. Kou, S. Shi, Dental pulp stem cells: from discovery to clinical application, J. Endod. 46 (9S) (2020) S46–S55, https://doi.org/10.1016/j.joen.2020.06.027.